

BNL--47931

DE92 040687

A Review of the Saturation Induced Harmonics in the 80 mm Aperture RHIC Arc Dipole Magnets

R. Gupta, P. Thompson and P. Wanderer

August 1992

DISCLAIMER

This report was prepared as an account of work sponsored by an agency of the United States Government. Neither the United States Government nor any agency thereof, nor any of their employees, makes any warranty, express or implied, or assumes any legal liability or responsibility for the accuracy, completeness, or usefulness of any information, apparatus, product, or process disclosed, or represents that its use would not infringe privately owned rights. Reference herein to any specific commercial product, process, or service by trade name, trademark, manufacturer, or otherwise does not necessarily constitute or imply its endorsement, recommendation, or favoring by the United States Government or any agency thereof. The views and opinions of authors expressed herein do not necessarily state or reflect those of the United States Government or any agency thereof.

R H I C P R O J E C T

Brookhaven National Laboratory
Associated Universities, Inc.
Upton, NY 11973

Under Contract No. DE-AC02-76CH00016 with the
UNITED STATES DEPARTMENT OF ENERGY

MASTER

SEP 10 1992

DISTRIBUTION OF THIS DOCUMENT IS UNLIMITED

A Review of the Saturation Induced Harmonics in the 80 mm Aperture RHIC Arc Dipole Magnets

R. Gupta, P. Thompson and P. Wanderer

1. Introduction

In this note we shall review, at times with a sense of history, the measured and computed saturation induced harmonics in the cross section of all long and short 80 mm aperture RHIC dipole magnets built so far. A somewhat similar study for a fewer magnets has been presented earlier in reference 1. With the help of several iterations in the yoke cross section, we have been able to reduce the saturation induced b_2 and b_4 harmonics by more than an order of magnitude. We shall briefly describe those iterations. The calculations described in this note have generally been done with the computer program POISSON. However, while comparing the calculations and measurements, we have included the results of field calculations with the code PE2D and MDP as well. The measurements are the average of up and down ramps. A small difference between the calculations and measurements has been observed consistently in the saturation induced b_2 and b_4 harmonics in all magnets DRA001 through DRA009. More work is still needed to explain the current dependence of skew quadrupole harmonic (a_1). We refer to current dependence of harmonics loosely as the saturation induced harmonics; but in an actual magnet it includes other effects like the harmonics induced by the coil deformation due to Lorentz forces, etc.

2. Measurements

In Fig. 2.1 through Fig. 2.4, we have summarized the measured current dependence of b_2 , b_4 , b_6 and a_1 harmonics in the 80 mm aperture RHIC dipoles built and tested to date. We present measurements only after 2 kAmp and they are the results of the averaging the up and down ramp. In order to make it easier to compare, we have shifted all harmonics to start them from a zero value at 2 kAmp. These measurements have been presented and discussed in detail earlier in various Testing and Measuring Group Notes by Wanderer², et.al. and in Magnet Division Notes by Thompson³.

One can note in Fig. 2.1 and Fig. 2.2 that the b_2 and b_4 saturation in the most recent dipole DRS6R (DRS006 Rebuilt with saturation suppressor hole) is significantly lower⁴ than in the earliest dipole DRA1 through DRA4. In DRA1 the maximum measured b_2 saturation till the design current of 5 kAmp was 43 unit; in contrast to that in DRS006R it is under 2 unit. Similarly, in DRA1 the maximum measured b_4 saturation till 5 kAmp current was 8.5 unit; in contrast in DRS6R it is under 0.5 unit. The b_6 saturation (Fig. 2.3) had a large fluctuations in the measurements in the earlier RHIC dipoles. It may have been -1 unit in DRA1; in magnet DRS6R, it is observed to be 1.2 unit maximum.

In Fig. 2.4, we have plotted the a_1 saturation in the long and short dipoles. It is clear that a large magnet to magnet variation has been observed both in the long and in the short dipoles. A current dependence is to be expected in the skew quadrupole harmonics (a_1) at high current when the flux lines can not be contained in the iron yoke and they start going through the low carbon steel cryostat which is asymmetrically located with respect to the magnet center. However, no current dependence was to be expected in the earlier long magnets which were located symmetrically in the cryostat and in the short dipoles which are not put inside a cryostat.

In Table 2.1 through Table 2.9, we have presented the numerical values of the harmonics plotted in Fig. 2.1 through Fig. 2.4 for each long magnet DRA001 through DRD009. We have not presented the short magnets as most of them were measured with a 30" coil. The 30" coil measurements in the short magnets not only reflect the measured harmonics in the straight section but also include the effects of the ends (coil length 36.9"), particularly in the iron saturation at high current where field lines tend to move more toward the two ends. The measurements with the 9" coils in magnets DRS006 and DRS008 have been described in detail in reference 4.

History of b2 Saturation in RHIC Dipoles

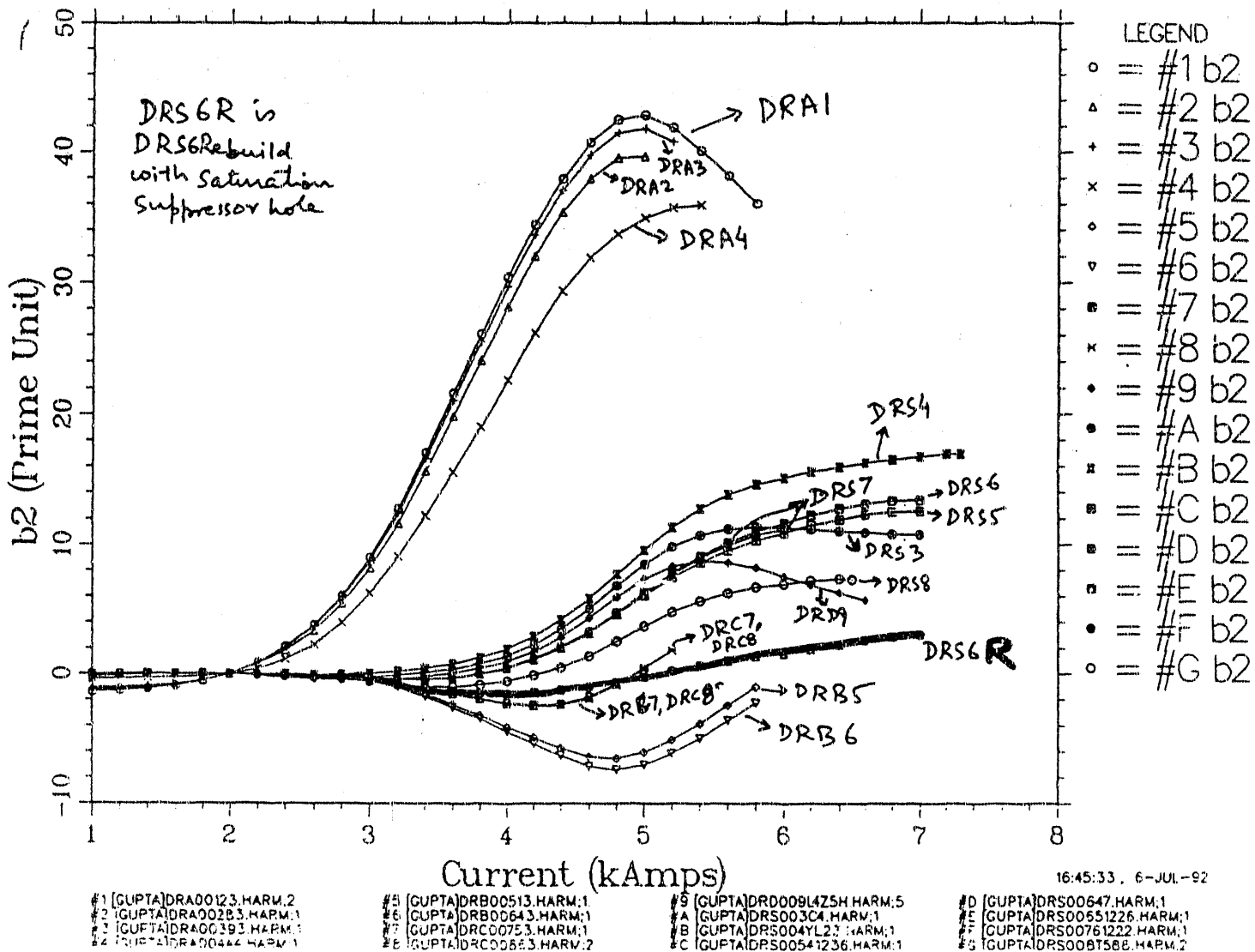


Figure 2.1: Measured current dependence of b_2 in various 80 mm aperture long and short dipoles for RHIC. The curves are the average of the up and down ramp and for each magnets they are shifted by an amount so that they start from zero at 3 kAmp.

History of b4 Saturation in RHIC Dipoles

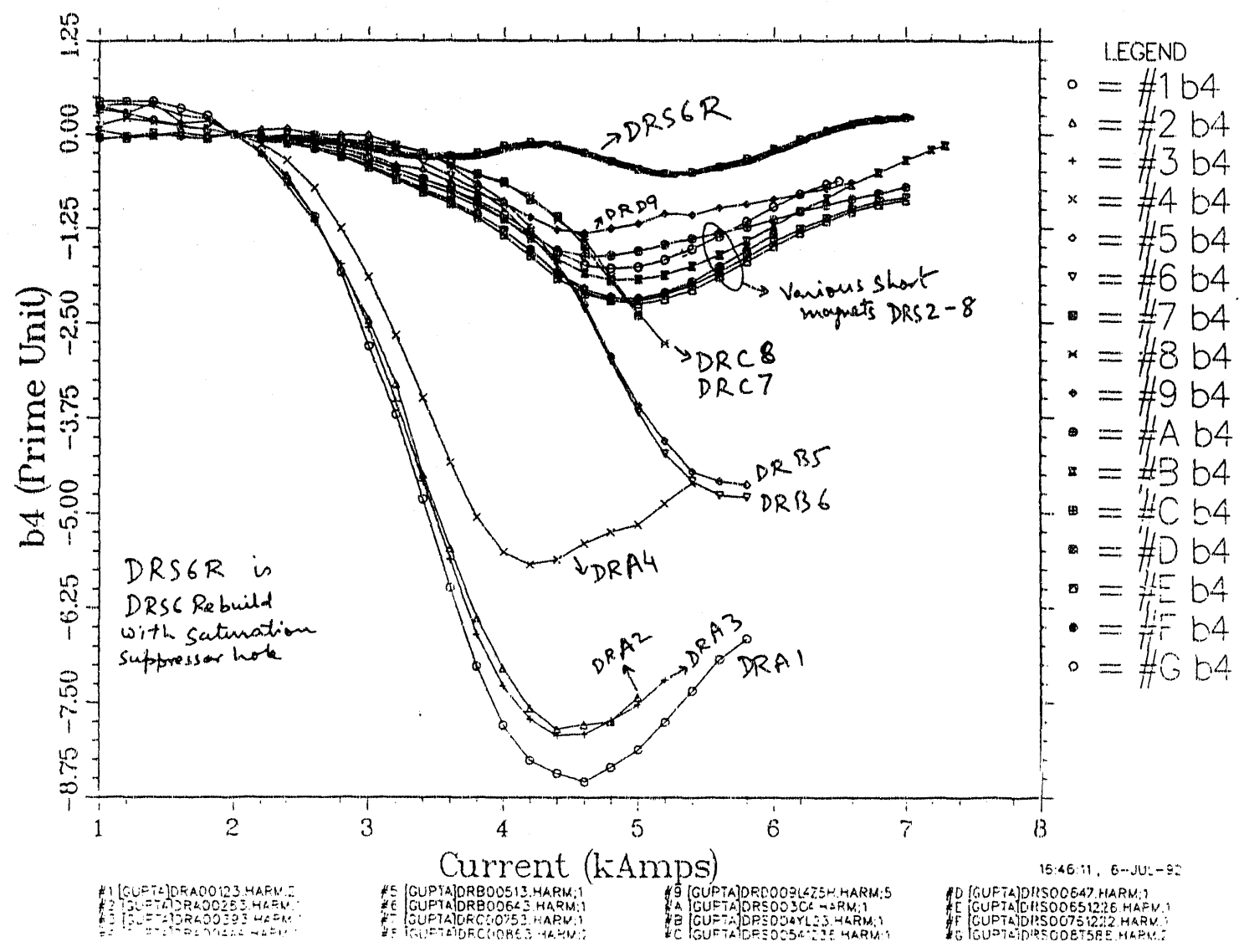


Figure 2.2: Measured current dependence of b_4 in various 80 mm aperture long and short dipoles for RHIC. The curves are the average of the up and down ramp and for each magnets they are shifted by an amount so that they start from zero at 2 kAmp.

History of b6 Saturation in RHIC Dipoles

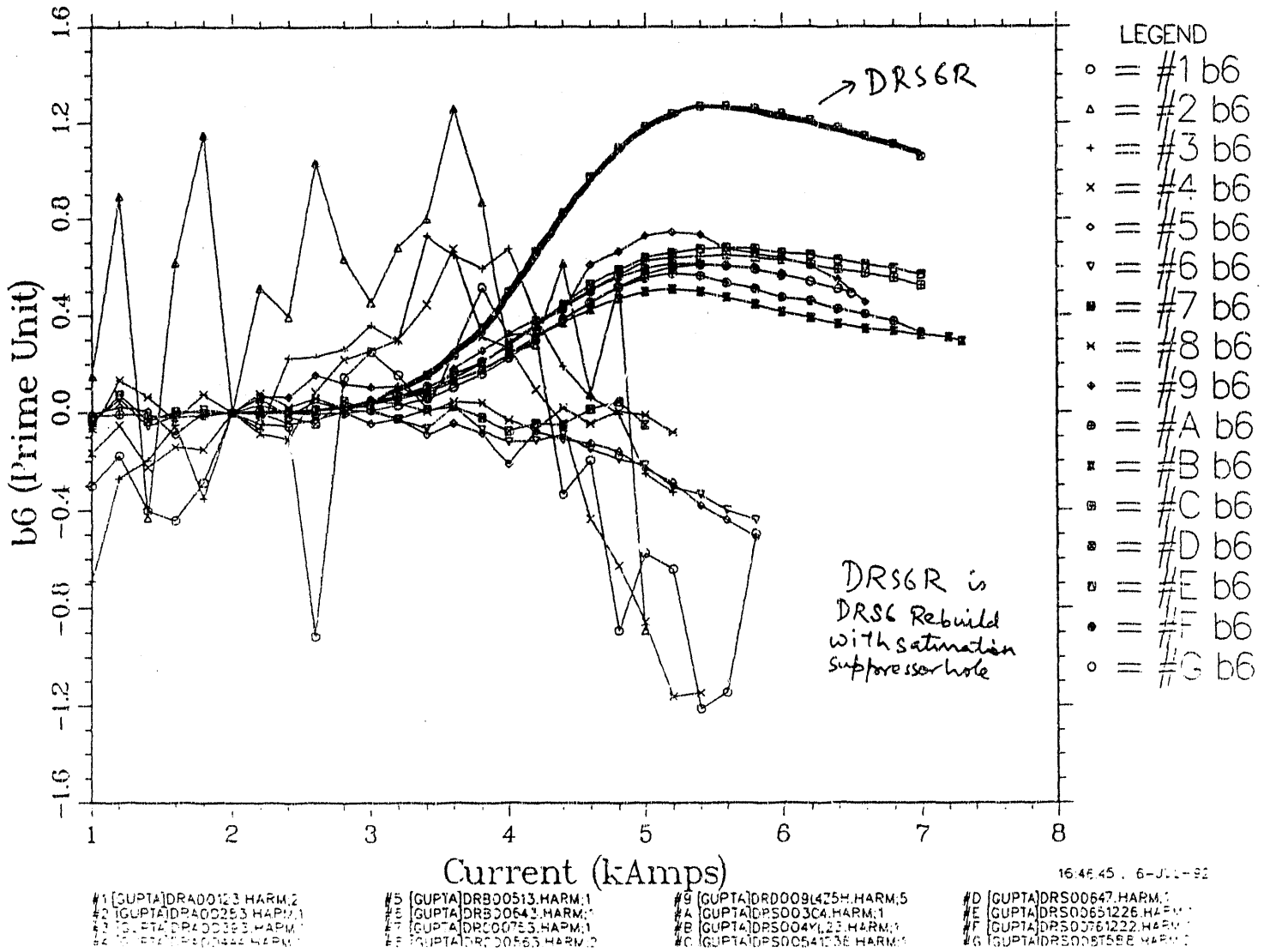


Figure 2.3: Measured current dependence of b_6 in various 80 mm aperture long and short dipoles for RHIC. The curves are the average of the up and down ramp and for each magnets they are shifted by an amount so that they start from zero at 2 kAmp.

History of a_1 Saturation in RHIC Dipoles

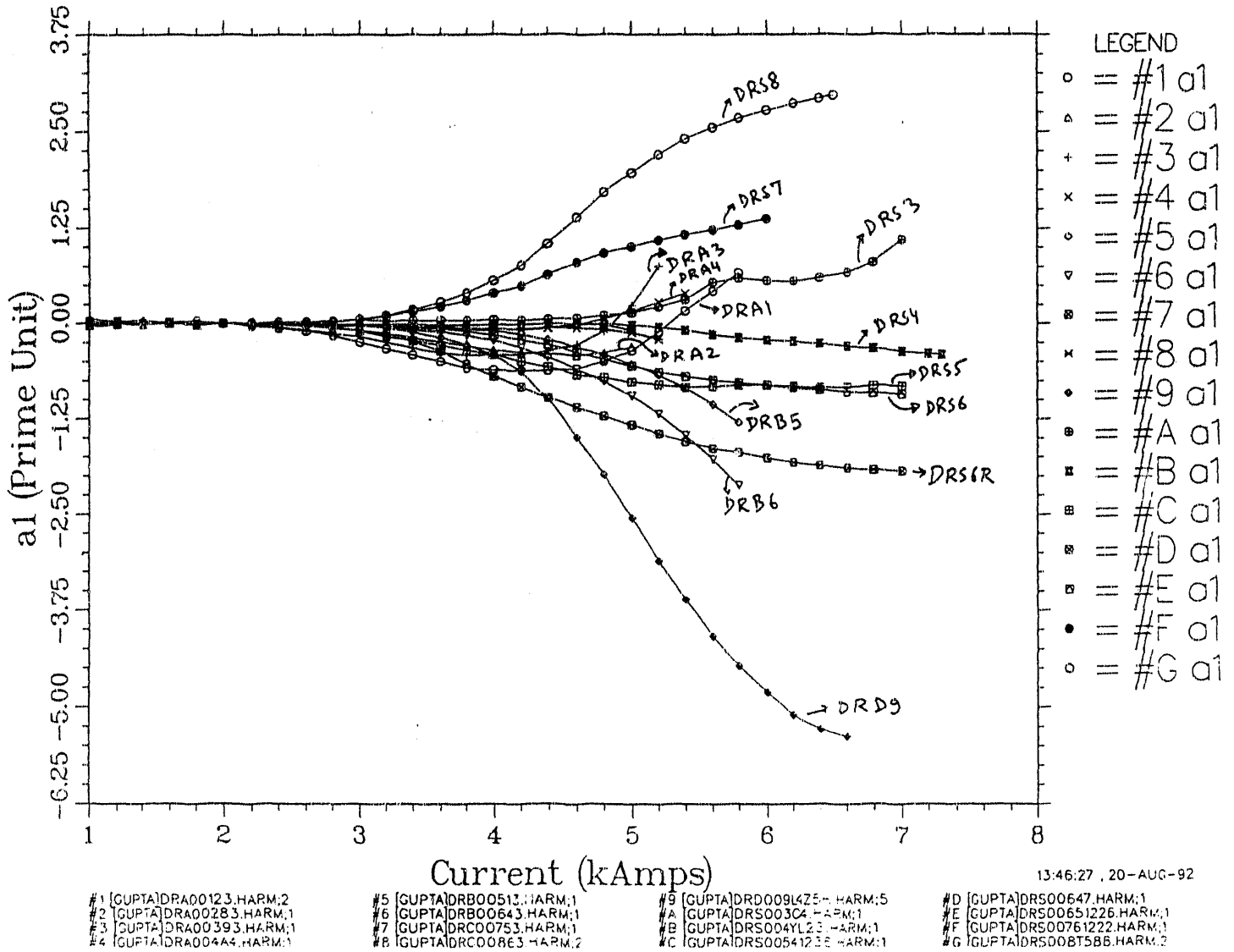


Figure 2.4: Measured current dependence of a_1 in various 80 mm aperture long and short dipoles for RHIC. The curves are the average of the up and down ramp and for each magnets they are shifted by an amount so that they start from zero at 2 kAmp.

Table 2.1: Average of the up and down ramp in the magnet DRA001. Moreover the harmonics are subtracted by the value of this average at 2 kAmp so that they have a zero value at 2kAmp. Please see the following processing for the details : DRA001.24023 27-APR-92 12:22:20

I kAmp	T.F. T/kA	δTF %	b'_2 10^{-4}	b'_4 10^{-4}	b'_6 10^{-4}	a'_1 10^{-4}
1.000	0.7702	0.069	-1.395	0.450	-0.300	0.015
1.200	0.7700	0.049	-1.270	0.440	-0.175	0.010
1.400	0.7700	0.047	-1.135	0.445	-0.400	0.015
1.600	0.7699	0.033	-0.905	0.345	-0.440	0.020
1.800	0.7698	0.025	-0.570	0.250	-0.285	0.040
2.000	0.7696	0.000	0.000	0.000	0.000	0.000
2.200	0.7694	-0.025	0.860	-0.220	-0.045	-0.030
2.400	0.7695	-0.023	2.080	-0.610	-0.055	-0.065
2.600	0.7690	-0.084	3.770	-1.105	-0.915	-0.095
2.800	0.7687	-0.124	6.005	-1.830	0.145	-0.155
3.000	0.7680	-0.217	9.005	-2.810	0.250	-0.245
3.200	0.7674	-0.290	12.725	-3.710	0.155	-0.325
3.400	0.7665	-0.401	17.035	-4.815	0.015	-0.410
3.600	0.7652	-0.582	21.605	-5.985	0.240	-0.495
3.800	0.7633	-0.825	26.095	-7.015	0.515	-0.580
4.000	0.7609	-1.129	30.430	-7.795	0.320	-0.610
4.200	0.7583	-1.477	34.425	-8.265	0.325	-0.615
4.400	0.7549	-1.910	37.920	-8.430	-0.335	-0.615
4.600	0.7517	-2.336	40.730	-8.545	-0.195	-0.585
4.800	0.7476	-2.862	42.470	-8.360	-0.890	-0.500
5.000	0.7433	-3.421	42.840	-8.120	-0.575	-0.355
5.200	0.7383	-4.072	41.855	-7.760	-0.640	-0.110
5.400	0.7328	-4.780	40.095	-7.340	-1.210	0.165
5.600	0.7273	-5.497	38.205	-6.925	-1.145	0.430
5.800	0.7215	-6.249	36.015	-6.655	-0.495	0.665

Table 2.2: Average of the up and down ramp in the magnet DRA002. Moreover the harmonics are subtracted by the value of this average at 2 kAmp so that they have a zero value at 2kAmp. Please see the following processing for the details : DRA002.23583 28-APR-92 09:25:43

I kAmp	T.F. T/kA	δTF %	b'_2 10^{-4}	b'_4 10^{-4}	b'_6 10^{-4}	a'_1 10^{-4}
1.000	0.7698	0.027	-1.080	0.340	0.150	-0.035
1.200	0.7697	0.016	-1.000	0.280	0.895	-0.010
1.400	0.7695	-0.010	-0.935	0.420	-0.430	-0.015
1.600	0.7695	-0.013	-0.765	0.150	0.620	0.000
1.800	0.7692	-0.049	-0.505	0.175	1.150	-0.015
2.000	0.7696	0.000	0.000	0.000	0.000	0.000
2.200	0.7692	-0.050	0.760	-0.250	0.515	-0.005
2.400	0.7685	-0.139	1.815	-0.555	0.395	-0.025
2.600	0.7686	-0.132	3.345	-1.110	1.035	-0.040
2.800	0.7682	-0.185	5.425	-1.765	0.635	-0.065
3.000	0.7679	-0.220	8.170	-2.460	0.455	-0.085
3.200	0.7668	-0.364	11.605	-3.310	0.680	-0.130
3.400	0.7657	-0.503	15.610	-4.495	0.800	-0.185
3.600	0.7643	-0.581	19.870	-5.470	1.260	-0.240
3.800	0.7626	-0.914	24.100	-6.385	0.870	-0.290
4.000	0.7605	-1.175	28.200	-7.040	0.245	-0.350
4.200	0.7576	-1.558	32.020	-7.575	0.280	-0.375
4.400	0.7547	-1.940	35.365	-7.850	0.615	-0.400
4.600	0.7508	-2.440	37.960	-7.790	0.075	-0.415
4.800	0.7469	-2.950	39.535	-7.750	0.530	-0.385
5.000	0.7427	-3.500	39.655	-7.425	-0.890	-0.305

Table 2.3: Average of the up and down ramp in the magnet DRA003. Moreover the harmonics are subtracted by the value of this average at 2 kAmp so that they have a zero value at 2kAmp. Please see the following processing for the details : DRA003.22993 28-APR-92 09:36:51

I kAmp	T.F. T/kA	δTF %	b'_2 10^{-4}	b'_4 10^{-4}	b'_6 10^{-4}	a'_1 10^{-4}
1.000	0.7696	0.076	-1.215	0.385	-0.690	-0.045
1.200	0.7691	0.015	-1.155	0.405	-0.270	-0.015
1.400	0.7693	0.032	-1.035	0.375	-0.195	0.000
1.600	0.7696	0.076	-0.855	0.255	-0.050	0.015
1.800	0.7691	0.016	-0.545	0.215	-0.350	0.005
2.000	0.7690	0.000	0.000	0.000	0.000	0.000
2.200	0.7691	0.006	0.850	-0.275	-0.065	-0.025
2.400	0.7688	-0.033	2.015	-0.685	0.225	-0.050
2.600	0.7688	-0.026	3.665	-1.180	0.230	-0.085
2.800	0.7683	-0.092	5.840	-1.730	0.260	-0.125
3.000	0.7678	-0.159	8.760	-2.565	0.360	-0.170
3.200	0.7669	-0.280	12.380	-3.545	0.295	-0.240
3.400	0.7664	-0.344	16.600	-4.580	0.730	-0.320
3.600	0.7649	-0.539	21.080	-5.615	0.650	-0.380
3.800	0.7631	-0.769	25.520	-6.600	0.595	-0.415
4.000	0.7607	-1.087	29.745	-7.275	0.675	-0.415
4.200	0.7578	-1.465	33.640	-7.720	0.395	-0.405
4.400	0.7545	-1.884	37.055	-7.930	0.190	-0.365
4.600	0.7514	-2.293	39.760	-7.915	0.065	-0.275
4.800	0.7473	-2.824	41.435	-7.745	-0.005	-0.105
5.000	0.7430	-3.379	41.790	-7.525	-0.250	0.240
5.200	0.7379	-4.041	40.780	-7.200	-0.325	0.755

Table 2.4: Average of the up and down ramp in the magnet DRA004. Moreover the harmonics are subtracted by the value of this average at 2 kAmp so that they have a zero value at 2kAmp. Please see the following processing for the details : DRA004.243A4 28-APR-92 09:42:54

I kAmp	T.F. T/kA	δTF %	b'_2 10^{-4}	b'_4 10^{-4}	b'_6 10^{-4}	a'_1 10^{-4}
1.000	0.7721	0.005	-0.405	0.130	-0.165	0.000
1.200	0.7720	-0.011	-0.350	0.210	-0.050	-0.005
1.400	0.7722	0.018	-0.315	0.165	-0.225	-0.010
1.600	0.7722	0.013	-0.270	0.100	-0.140	-0.005
1.800	0.7722	0.006	-0.185	0.075	-0.150	-0.020
2.000	0.7721	0.000	0.000	0.000	0.000	0.000
2.200	0.7720	-0.017	0.380	-0.130	-0.085	-0.005
2.400	0.7718	-0.045	1.110	-0.355	-0.110	-0.005
2.600	0.7715	-0.079	2.245	-0.725	0.085	-0.010
2.800	0.7713	-0.105	3.925	-1.255	0.220	-0.020
3.000	0.7708	-0.174	6.230	-1.900	0.255	-0.030
3.200	0.7699	-0.289	9.970	-2.670	0.300	-0.030
3.400	0.7691	-0.390	12.230	-3.490	0.445	-0.035
3.600	0.7676	-0.588	15.545	-4.340	0.675	-0.045
3.800	0.7660	-0.789	19.010	-5.055	0.315	-0.060
4.000	0.7636	-1.103	22.635	-5.515	0.270	-0.065
4.200	0.7611	-1.422	26.180	-5.680	0.095	-0.085
4.400	0.7580	-1.826	29.350	-5.615	-0.045	-0.065
4.600	0.7543	-2.301	31.900	-5.400	-0.435	-0.010
4.800	0.7502	-2.841	33.680	-5.255	-0.625	0.060
5.000	0.7455	-3.451	34.935	-5.155	-0.855	0.160
5.200	0.7403	-4.113	35.700	-4.880	-1.160	0.280
5.400	0.7349	-4.813	35.940	-4.605	-1.145	0.395

Table 2.5: Average of the up and down ramp in the magnet DRB005. Moreover the harmonics are subtracted by the value of this average at 2 kAmp so that they have a zero value at 2kAmp. Please see the following processing for the details : DRB005.25013 27-APR-92 11:13:36

I kAmp	T.F. T/kA	δTF %	b'_2 10^{-4}	b'_4 10^{-4}	b'_6 10^{-4}	a'_1 10^{-4}
1.000	0.7073	0.035	-0.100	-0.075	-0.005	0.055
1.200	0.7073	0.029	-0.055	-0.030	0.025	0.035
1.400	0.7072	0.016	-0.010	-0.020	0.005	0.040
1.600	0.7072	0.019	0.000	0.025	-0.090	0.020
1.800	0.7070	-0.004	0.010	-0.025	0.000	0.010
2.000	0.7071	0.000	0.000	0.000	0.000	0.000
2.200	0.7071	0.001	-0.025	0.055	0.000	-0.005
2.400	0.7069	-0.025	-0.045	0.070	-0.045	-0.010
2.600	0.7069	-0.028	-0.075	-0.005	-0.030	-0.010
2.800	0.7068	-0.042	-0.175	-0.010	0.005	-0.010
3.000	0.7066	-0.058	-0.410	-0.015	-0.045	-0.020
3.200	0.7063	-0.111	-0.875	-0.140	-0.025	-0.020
3.400	0.7057	-0.187	-1.570	-0.240	-0.090	-0.040
3.600	0.7049	-0.311	-2.360	-0.440	-0.045	-0.055
3.800	0.7039	-0.442	-3.205	-0.670	-0.085	-0.075
4.000	0.7029	-0.582	-4.080	-0.895	-0.210	-0.100
4.200	0.7014	-0.798	-4.930	-1.245	-0.075	-0.140
4.400	0.6994	-1.081	-5.715	-1.705	-0.110	-0.215
4.600	0.6969	-1.432	-6.395	-2.245	-0.125	-0.305
4.800	0.6937	-1.881	-6.550	-2.945	-0.160	-0.405
5.000	0.6906	-2.331	-6.065	-3.590	-0.230	-0.530
5.200	0.6872	-2.803	-5.110	-4.060	-0.285	-0.675
5.400	0.6835	-3.334	-3.845	-4.460	-0.380	-0.845
5.600	0.6796	-3.878	-2.445	-4.585	-0.440	-1.060
5.800	0.6753	-4.494	-1.055	-4.630	-0.510	-1.300

Table 2.6: Average of the up and down ramp in the magnet DRB006. Moreover the harmonics are subtracted by the value of this average at 2 kAmp so that they have a zero value at 2kAmp. Please see the following processing for the details : DRB006.22743 27-APR-92 14:09:46

I kAmp	T.F. T/kA	δTF %	b_2 10^{-4}	b_4 10^{-4}	b_6 10^{-4}	a_1 10^{-4}
1.000	0.7082	0.019	-0.010	-0.055	-0.040	0.025
1.200	0.7082	0.012	0.015	-0.030	0.060	0.030
1.400	0.7084	0.048	0.030	0.015	-0.055	0.010
1.600	0.7078	-0.047	0.040	-0.040	-0.010	0.020
1.800	0.7077	-0.043	0.010	-0.055	0.015	0.010
2.000	0.7081	0.000	0.000	0.000	0.000	0.000
2.200	0.7082	0.016	-0.035	-0.055	0.035	-0.005
2.400	0.7080	-0.019	-0.085	0.000	-0.005	-0.010
2.600	0.7073	-0.064	-0.165	-0.075	0.045	-0.015
2.800	0.7072	-0.124	-0.310	-0.075	0.015	-0.025
3.000	0.7071	-0.144	-0.585	-0.135	0.005	-0.030
3.200	0.7071	-0.144	-1.065	-0.200	-0.025	-0.045
3.400	0.7068	-0.181	-1.765	-0.380	-0.065	-0.080
3.600	0.7060	-0.294	-2.585	-0.565	0.025	-0.105
3.800	0.7052	-0.407	-3.485	-0.750	-0.070	-0.155
4.000	0.7042	-0.544	-4.440	-0.995	-0.120	-0.225
4.200	0.7022	-0.832	-5.380	-1.345	-0.115	-0.310
4.400	0.7004	-1.092	-6.300	-1.735	-0.090	-0.450
4.600	0.6983	-1.387	-7.130	-2.310	-0.150	-0.590
4.800	0.6950	-1.842	-7.420	-3.005	-0.190	-0.760
5.000	0.6917	-2.310	-7.055	-3.680	-0.215	-0.945
5.200	0.6889	-2.711	-6.180	-4.225	-0.305	-1.185
5.400	0.6853	-3.211	-4.990	-4.580	-0.335	-1.470
5.600	0.6806	-3.876	-3.615	-4.770	-0.400	-1.785
5.800	0.6767	-4.438	-2.305	-4.795	-0.440	-2.125

Table 2.7: Average of the up and down ramp in the magnet DRC007. Moreover the harmonics are subtracted by the value of this average at 2 kAmp so that they have a zero value at 2kAmp. Please see the following processing for the details : DRC007.23553 27-APR-92 14:36:35

I kAmp	T.F. T/kA	δTF %	b_2' 10^{-4}	b_4' 10^{-4}	b_6' 10^{-4}	a_1' 10^{-4}
1.000	0.7087	0.050	-0.085	-0.040	-0.040	-0.015
1.200	0.7086	0.023	-0.025	-0.055	0.075	0.000
1.400	0.7085	0.025	0.000	-0.020	-0.035	0.000
1.600	0.7085	0.020	0.010	-0.020	0.005	-0.005
1.800	0.7085	0.016	0.025	-0.065	0.000	-0.005
2.000	0.7084	0.000	0.000	0.000	0.000	0.000
2.200	0.7084	0.002	-0.005	-0.075	0.060	0.005
2.400	0.7083	-0.009	-0.050	-0.010	-0.015	-0.005
2.600	0.7081	-0.038	-0.100	-0.025	-0.045	0.000
2.800	0.7081	-0.040	-0.195	-0.075	0.050	-0.005
3.000	0.7079	-0.070	-0.370	-0.100	0.015	-0.005
3.200	0.7077	-0.099	-0.680	-0.150	-0.025	-0.005
3.400	0.7073	-0.144	-1.100	-0.255	0.015	-0.010
3.600	0.7067	-0.228	-1.525	-0.400	0.025	-0.015
3.800	0.7063	-0.293	-1.915	-0.540	-0.020	-0.015
4.000	0.7053	-0.426	-2.250	-0.640	-0.075	-0.015
4.200	0.7041	-0.599	-2.415	-0.875	-0.045	-0.005
4.400	0.7026	-0.818	-2.345	-1.095	-0.050	-0.005
4.600	0.7005	-1.103	-1.800	-1.490	0.015	-0.005
4.800	0.6980	-1.467	-0.775	-1.950	0.045	-0.020
5.000	0.6950	-1.883	0.345	-2.400	-0.050	-0.080

Table 2.8: Average of the up and down ramp in the magnet DRC008. Moreover the harmonics are subtracted by the value of this average at 2 kAmp so that they have a zero value at 2kAmp. Please see the following processing for the details : DRC008.25463 27-APR-92 14:57:02

I kAmp	T.F. T/kA	δTF %	b'_2 10^{-4}	b'_4 10^{-4}	b'_6 10^{-4}	a'_1 10^{-4}
1.000	0.7086	0.035	-0.080	0.060	-0.065	-0.005
1.200	0.7086	0.036	-0.010	-0.020	0.135	0.010
1.400	0.7084	0.018	0.025	-0.030	0.065	0.010
1.600	0.7086	0.038	0.025	0.025	-0.030	0.000
1.800	0.7084	0.011	0.015	-0.030	0.075	0.005
2.000	0.7083	0.000	0.000	0.000	0.000	0.000
2.200	0.7082	-0.014	-0.020	-0.025	0.080	0.000
2.400	0.7081	-0.030	-0.055	-0.015	0.025	-0.015
2.600	0.7081	-0.036	-0.110	-0.045	0.060	-0.025
2.800	0.7079	-0.060	-0.210	-0.080	0.020	-0.030
3.000	0.7079	-0.061	-0.395	-0.095	0.045	-0.040
3.200	0.7075	-0.112	-0.710	-0.170	0.040	-0.045
3.400	0.7072	-0.159	-1.140	-0.255	0.005	-0.065
3.600	0.7067	-0.231	-1.565	-0.410	0.045	-0.065
3.800	0.7060	-0.323	-1.970	-0.550	0.040	-0.075
4.000	0.7052	-0.433	-2.310	-0.665	-0.030	-0.075
4.200	0.7041	-0.600	-2.505	-0.825	-0.070	-0.065
4.400	0.7024	-0.831	-2.445	-1.140	0.020	-0.060
4.600	0.7004	-1.112	-1.915	-1.400	-0.045	-0.055
4.800	0.6980	-1.450	-0.880	-1.895	0.005	-0.080
5.000	0.6951	-1.868	0.465	-2.370	-0.010	-0.120
5.200	0.6918	-2.326	1.815	-2.775	-0.080	-0.205

Table 2.9: Average of the up and down ramp in the magnet DRD009. Moreover the harmonics are subtracted by the value of this average at 2 kAmp so that they have a zero value at 2kAmp. Please see the following processing for the details : DRD009.101L4 30-APR-92 14:08:26

I kAmp	T.F. T/kA	δTF %	b'_2 10^{-4}	b'_4 10^{-4}	b'_6 10^{-4}	a'_1 10^{-4}
2.000	0.7076	0.000	0.000	0.000	0.000	0.000
2.200	0.7074	-0.022	-0.145	-0.050	0.065	-0.015
2.400	0.7073	-0.032	-0.290	-0.060	0.065	-0.010
2.600	0.7071	-0.063	-0.405	-0.145	0.155	-0.005
2.800	0.7069	-0.092	-0.480	-0.205	0.120	-0.020
3.000	0.7066	-0.134	-0.480	-0.280	0.105	-0.030
3.200	0.7063	-0.187	-0.400	-0.420	0.110	-0.055
3.400	0.7057	-0.266	-0.230	-0.475	0.055	-0.110
3.600	0.7047	-0.411	0.050	-0.650	0.180	-0.185
3.800	0.7036	-0.568	0.425	-0.795	0.255	-0.275
4.000	0.7021	-0.772	0.960	-0.910	0.325	-0.415
4.200	0.7002	-1.037	1.730	-1.110	0.385	-0.625
4.400	0.6979	-1.368	2.840	-1.270	0.415	-0.985
4.600	0.6950	-1.780	4.330	-1.320	0.610	-1.490
4.800	0.6917	-2.239	5.925	-1.265	0.665	-1.985
5.000	0.6883	-2.731	7.330	-1.195	0.730	-2.545
5.200	0.6845	-3.261	8.325	-1.060	0.745	-3.110
5.400	0.6805	-3.824	8.730	-1.080	0.735	-3.610
5.600	0.6763	-4.418	8.610	-0.985	0.675	-4.085
5.800	0.6720	-5.022	8.175	-0.935	0.655	-4.470
6.000	0.6676	-5.647	7.535	-0.870	0.640	-4.810
6.200	0.6632	-6.273	6.875	-0.795	0.605	-5.100
6.400	0.6589	-6.880	6.275	-0.725	0.550	-5.285
6.600	0.6547	-7.477	5.675	-0.645	0.455	-5.375

3. Calculations

In this section we present the results of the POISSON calculations for all long magnets built and tested so far, namely DRA001 through DRD009. We have ignored the effect of cryostat wall on field harmonics, which is present in all long magnets. The most recent short magnets are discussed in reference 4. Just as in the case of measurements, we have shifted the harmonics to start them from zero, however, in the case of calculations they are made zero at zero current (i.e., for $\infty\mu$ calculations) instead of 2 kA.

The magnets DRA001, DRA002 and DRA003 were built at BBC with an identical iron cross section. A POISSON model for them is shown in Fig. 3.1 and the results of calculations are given in Table 3.1. These magnets have a 5 mm gap between the coil and yoke. The POISSON model is made as per the drawings obtained from BBC.

The magnet DRA004 was built at BNL with some modifications in the the DRA003 cross section. A POISSON model for DRA004 is shown in Fig. 3.2 and the results of calculations are given in Table 3.2. This magnet also has a 5 mm gap between the coil and yoke. The iron yoke model is based on the drawing No. 22-242.04-4 Revision B.

The magnets DRB005 and DRB006 were built at BNL with an identical iron cross section. A POISSON model for them is shown in Fig. 3.3 and the results of calculations are given in Table 3.3. These magnets have a 10 mm gap between the coil and yoke. The yoke model is based on the drawing No. 22-398.05-5. The key is made of non-magnetic stainless steel.

The magnets DRC007 and DRC008 were built at BNL with an identical iron cross section. A POISSON model for them is shown in Fig. 3.4 and the results of calculations are given in Table 3.4. These magnets have a 10 mm gap between the coil and yoke. As in the case of DRB005, the iron model is based on the drawing No. 22-398.05-5. The only difference between the DRB005 (or DRB006) and DRC007 (or DRC008) is that the key material is changed from non-magnetic stainless steel to low carbon magnet steel.

The magnet DRD009 was built at BNL with a new iron cross section. A POISSON model for it is shown in Fig. 3.5 and the results of calculations are given in Table 3.5. This magnet, like all other dipoles starting from DRB005, has a 10 mm gap between the coil and the yoke. The POISSON model for the yoke is based on the drawing No. 22-714.02-5 Revision A.

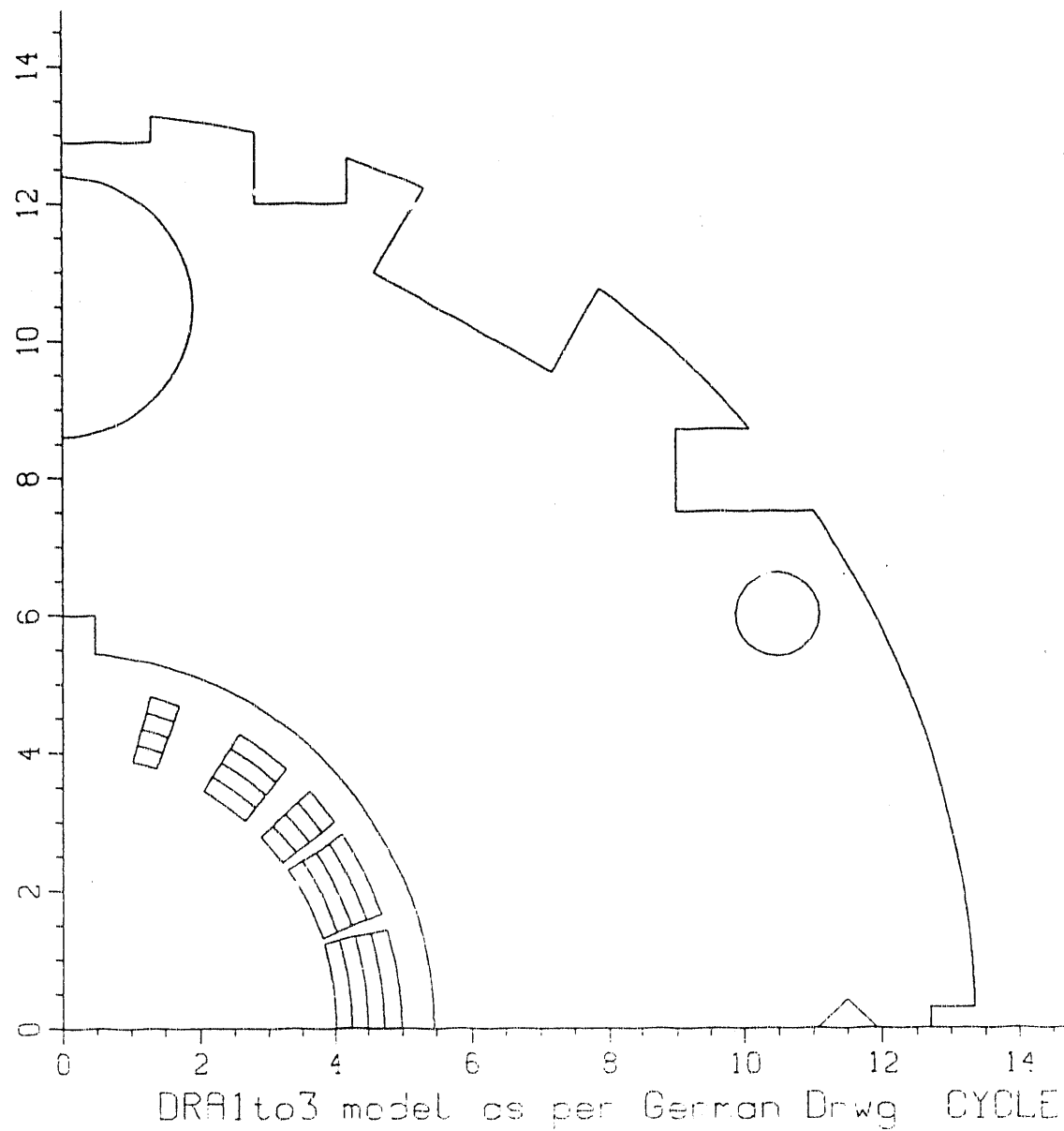


Figure 3.1: POISSON model for the 80 mm aperture RHIC arc dipole magnets DRA001, DRA002 and DRA003. The model is made as per the drawings obtained from BBC.

Table 3.1: Results of POISSON calculations for magnets DRA001, DRA002 and DRA003. The result file is DRA123.LOG;4.

I kAmp	B_o Tesla	T.F. T/kA	b'_2 10^{-4}	b'_4 10^{-4}	b'_6 10^{-4}	b'_8 10^{-4}	b'_{10} 10^{-4}	b'_{12} 10^{-4}
0.000	0.0000	0.00000	0.000	0.000	0.000	0.000	0.000	0.000
2.000	1.5102	-0.03071	0.237	-0.073	0.022	-0.003	0.000	0.000
3.000	2.2622	-0.16619	6.257	-1.835	0.405	-0.078	0.014	-0.001
4.000	2.9899	-1.04152	24.994	-6.354	0.732	-0.070	0.000	0.008
4.500	3.3305	-2.01454	34.027	-7.150	0.209	0.029	-0.010	0.014
5.000	3.6479	-3.41015	35.953	-6.971	-0.449	0.065	-0.015	0.024
5.500	3.9362	-5.25105	32.215	-6.131	-0.727	0.116	-0.016	0.037
6.000	4.2058	-7.19666	27.423	-5.170	-0.812	0.159	-0.019	0.052
7.000	4.7095	-10.92848	18.742	-3.643	-0.899	0.192	-0.030	0.079
8.000	5.1882	-14.14024	13.319	-2.283	-0.946	0.208	-0.040	0.103

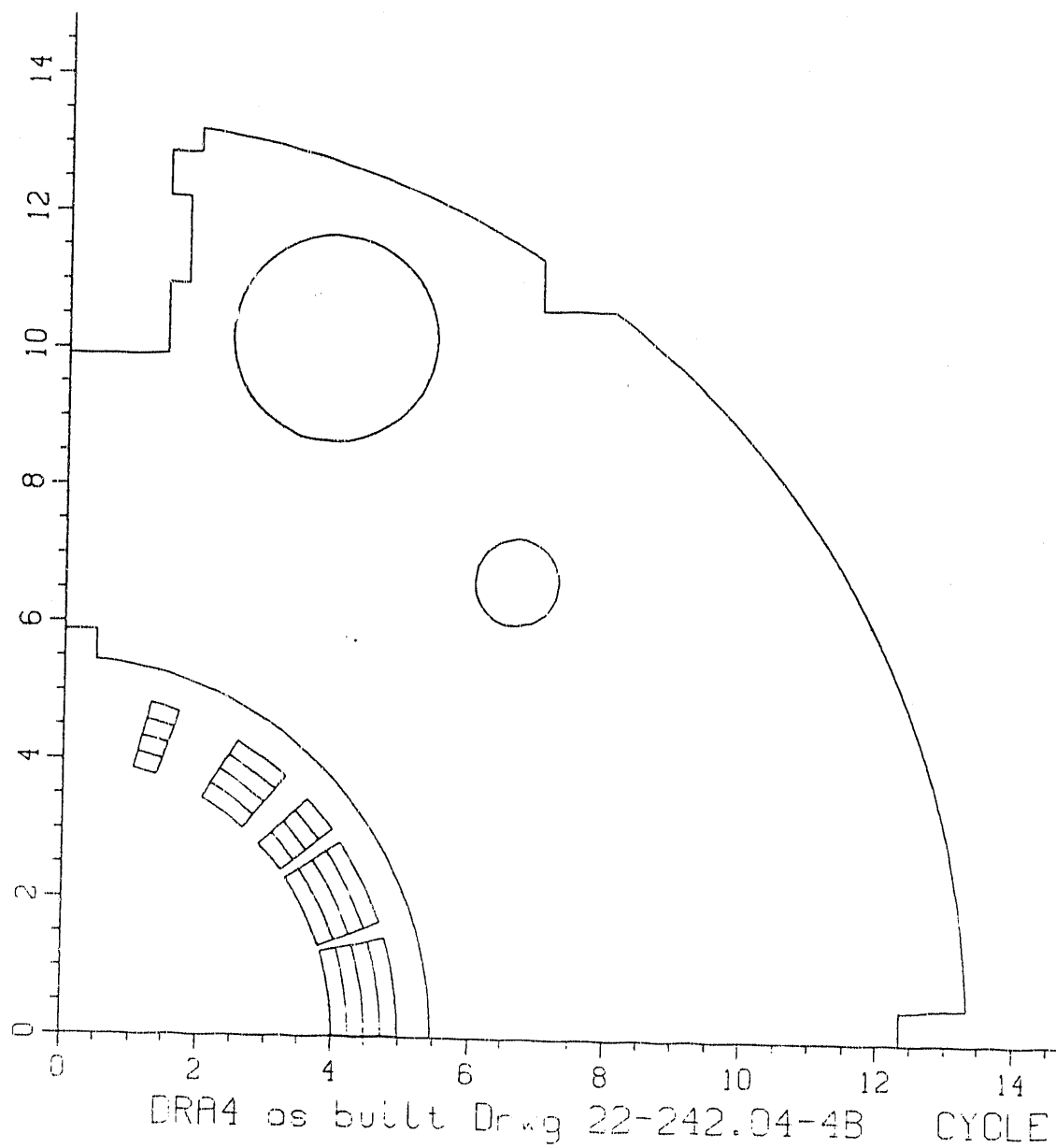


Figure 3.2: POISSON model for the 80 mm aperture RHIC arc dipole magnet DRA004. The iron yoke model is based on the drawing No. 22-242.04-4 Revision B.

Table 3.2: Results of POISSON calculations for magnet DRA004. The result file is DRA4.LOG;5.

I kAmp	B_o Tesla	T.F. T/kA	b'_2 10^{-4}	b'_4 10^{-4}	b'_6 10^{-4}	b'_8 10^{-4}	b'_{10} 10^{-4}	b'_{12} 10^{-4}
0.000	0.0000	0.00000	0.000	0.000	0.000	0.000	0.000	0.000
1.000	0.7551	-0.02383	0.041	0.004	0.003	0.001	0.000	0.000
2.000	1.5101	-0.03165	0.245	-0.063	0.021	-0.003	0.000	0.000
3.000	2.2625	-0.15058	5.678	-1.623	0.363	-0.071	0.013	-0.001
4.500	3.3411	-1.70004	32.365	-5.865	-0.018	0.026	-0.015	0.013
5.000	3.6617	-3.04059	35.491	-5.797	-0.798	0.029	-0.029	0.022
5.500	3.9565	-4.75846	35.453	-5.272	-1.318	-0.003	-0.045	0.033
6.000	4.2283	-6.69863	34.234	-4.161	-1.473	-0.011	-0.056	0.046
7.000	4.7250	-10.63282	25.556	-2.493	-1.430	0.046	-0.059	0.075
8.000	5.1998	-13.94705	17.941	-1.111	-1.315	0.109	-0.058	0.101

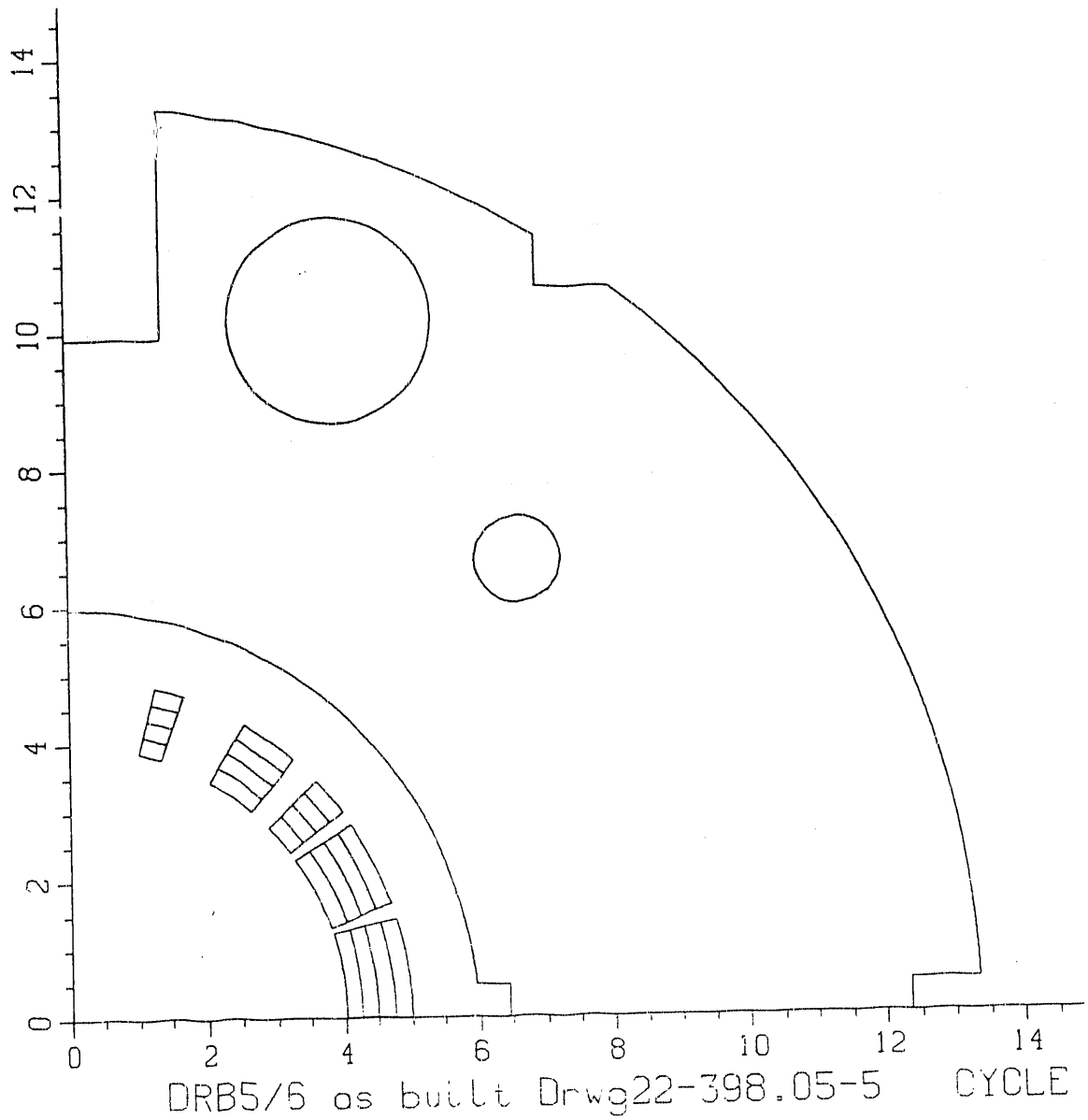


Figure 3.3: POISSON model for the 80 mm aperture RHIC arc dipole magnets DRB005 and DRB006. The yoke model is based on the drawing No. 22-398.05-5. The key is made of non-magnetic stainless steel.

Table 3.3: Results of POISSON calculations for magnets DRB005 and DRB006. The result file is DRB5.LOG;1.

I kAmp	B_o Tesla	T.F. T/kA	b'_2 10^{-4}	b'_4 10^{-4}	b'_6 10^{-4}	b'_8 10^{-4}	b'_{10} 10^{-4}	b'_{12} 10^{-4}
0.000	0.0000	0.00000	0.000	0.000	0.000	0.000	0.000	0.000
1.000	0.7074	-0.02261	0.020	0.001	0.003	0.001	-0.001	0.000
2.000	1.4148	-0.02600	-0.003	-0.002	0.001	0.001	0.000	0.000
3.000	2.1218	-0.04791	-0.196	-0.031	-0.003	-0.001	-0.001	0.000
4.000	2.8200	-0.36729	-3.051	-0.787	-0.103	-0.019	-0.004	0.002
4.500	3.1541	-0.94530	-6.476	-1.918	-0.208	-0.048	-0.008	0.005
5.000	3.4682	-1.97496	-8.774	-3.974	-0.383	-0.082	-0.015	0.010
5.500	3.7665	-3.22082	-7.239	-5.422	-0.599	-0.101	-0.020	0.017
6.000	4.0439	-4.75201	-5.051	-5.753	-0.748	-0.121	-0.022	0.026
7.000	4.5449	-8.24351	-5.612	-5.254	-0.791	-0.127	-0.020	0.051

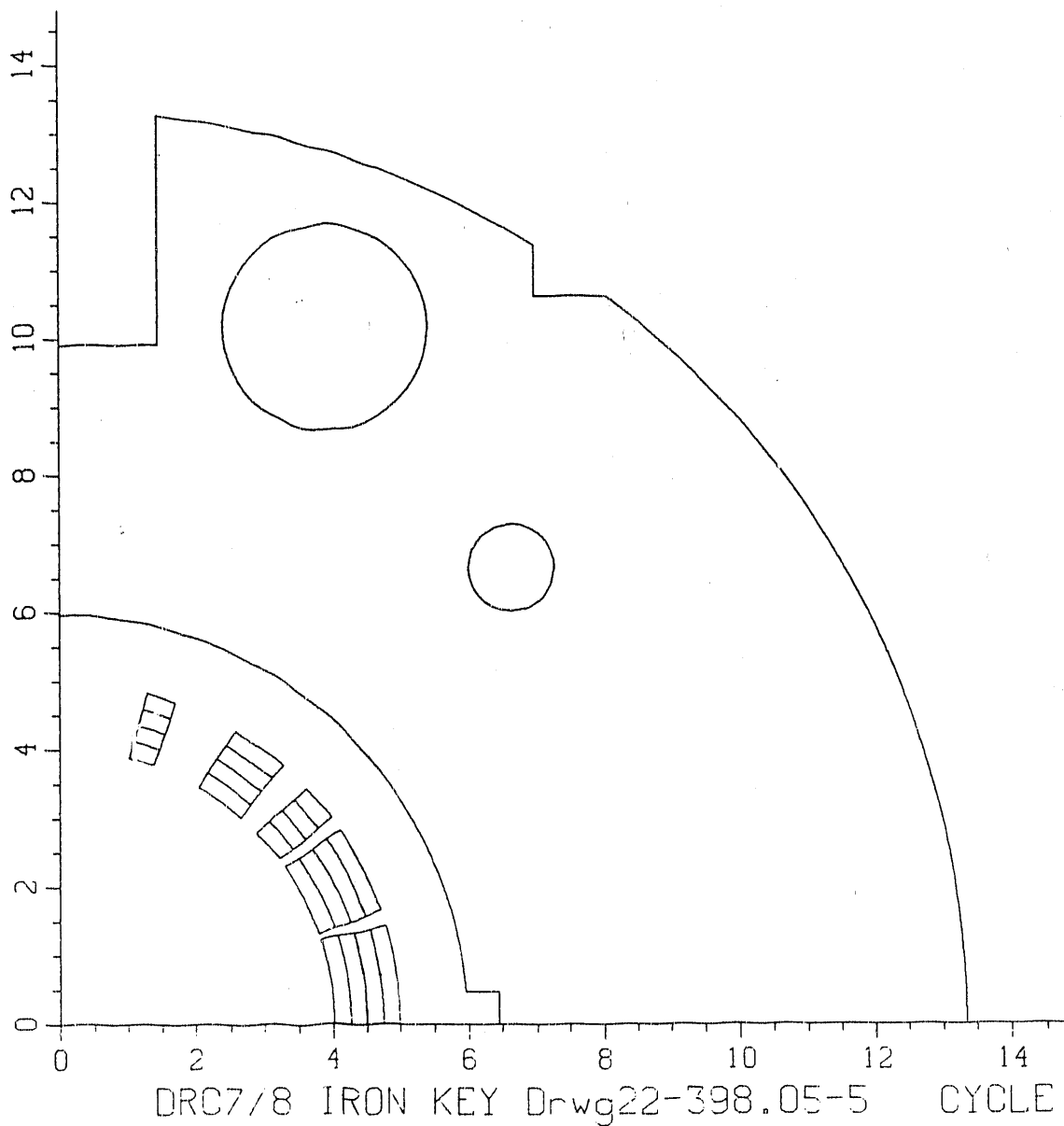


Figure 3.4: POISSON model for the 80 mm aperture RHIC arc dipole magnets DRC007 and DRC008. The iron model is based on the drawing No. 22-398.05-5. The yoke key is made of low carbon magnetic steel.

Table 3.4: Results of POISSON calculations for magnets DRC007 and DRC008. The result file is DRC7.log;2.

I kAmp	B_o Tesla	T.F. T/kA	b'_2 10^{-4}	b'_4 10^{-4}	b'_6 10^{-4}	b'_8 10^{-4}	b'_{10} 10^{-4}	b'_{12} 10^{-4}
0.000	0.0000	0.00000	0.000	0.000	0.000	0.000	0.000	0.000
1.000	0.7074	-0.02247	0.021	0.001	0.002	0.001	0.000	0.000
2.000	1.4149	-0.02530	0.003	-0.001	0.002	0.001	-0.001	0.000
3.000	2.1220	-0.03943	-0.053	-0.006	0.000	0.000	0.000	0.000
4.000	2.8240	-0.22915	-0.622	-0.376	-0.033	-0.007	-0.002	0.001
4.500	3.1628	-0.67301	-1.444	-1.073	-0.064	-0.026	-0.004	0.004
5.000	3.4851	-1.49560	0.751	-2.393	-0.119	-0.038	-0.008	0.008
5.500	3.7835	-2.78350	2.179	-3.804	-0.340	-0.060	-0.014	0.015
6.000	4.0558	-4.47243	1.595	-4.542	-0.556	-0.092	-0.018	0.025
7.000	4.5525	-8.09129	-1.519	-4.469	-0.665	-0.108	-0.017	0.050
7.500	4.7913	-9.71831	-2.708	-4.160	-0.637	-0.103	-0.016	0.062
8.000	5.0274	-11.18983	-3.509	-3.835	-0.601	-0.096	-0.014	0.073

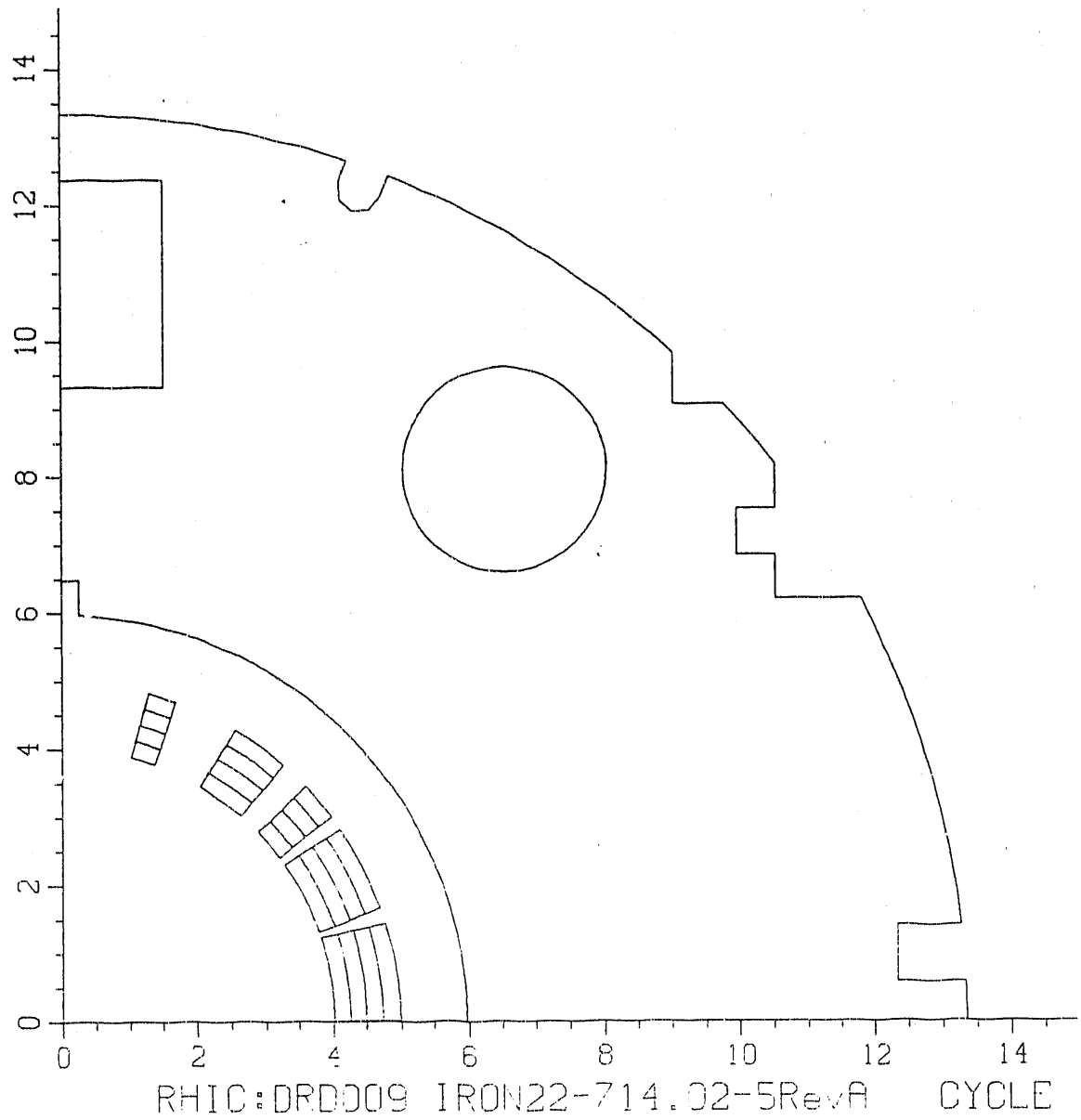


Figure 3.5: POISSON model for the 80 mm aperture RHIC arc dipole magnet DRD009. The yoke model is based on the drawing No. 22-714.02-5 Revision A.

Table 3.5: The results of POISSON calculations for the RHIC magnet DRD009. The results are stored on file DRD9.LOG;2.

I kAmp	B_0 Tesla	T.F. T/kA	b'_2 10^{-4}	b'_4 10^{-4}	b'_6 10^{-4}	b'_8 10^{-4}	b'_{10} 10^{-4}	b'_{12} 10^{-4}
0.000	0.0000	0.00000	0.000	0.000	0.000	0.000	0.000	0.000
1.415	1.0004	-0.02482	0.040	0.004	0.002	0.001	-0.001	0.000
2.000	1.4140	-0.02715	0.030	0.007	0.002	0.001	0.000	0.000
3.000	2.1200	-0.07239	0.533	-0.090	0.037	-0.007	0.001	0.000
4.000	2.8081	-0.72783	3.105	-0.437	0.243	-0.055	0.003	0.003
4.500	3.1306	-1.62474	6.527	-0.550	0.477	-0.095	0.001	0.008
4.750	3.2833	-2.25619	8.585	-0.442	0.582	-0.107	-0.005	0.012
5.000	3.4295	-3.00662	9.396	-0.446	0.618	-0.116	-0.010	0.017
5.250	3.5702	-3.83722	8.863	-0.563	0.599	-0.119	-0.015	0.022
5.500	3.7072	-4.68668	7.873	-0.635	0.567	-0.117	-0.018	0.027
6.000	3.9721	-6.38510	5.264	-0.602	0.511	-0.097	-0.018	0.039
7.000	4.4806	-9.48737	1.663	-0.380	0.381	-0.058	-0.013	0.061
8.000	4.9688	-12.17076	0.178	-0.333	0.254	-0.033	-0.009	0.082

4. Calculations versus Measurements

In this section we compare measurements and the calculations for the current dependence of the field harmonics (b_2 and b_4 only) in all long magnets. The calculations are done for the saturation induced harmonics with the computer codes POISSON, PE2D and MDP. The current dependence on the field harmonics may also come due to a small coil deformation as a result of the Lorentz force on the coil. This has not been included in the calculations. The b_6 harmonic could not be obtained to the desired accuracy in the earlier magnets (DRA001 through DRC008) to make any meaningful comparison. In the latest long magnet DRD009, the agreement between the calculations and measurements for the current dependence of b_6 is better than $\frac{1}{4}$ unit.

In Fig. 4.1 and Fig. 4.2 we have plotted computed and measured b_2 and b_4 as a function of current for the three magnets DRA001, DRA002 and DRA003, made with the same iron cross-section. The calculations are made with the code POISSON, PE2D and MDP.

In Fig. 4.3 and Fig. 4.4 we have done the same comparison between the calculations and measurements for the magnet DRA004. The calculations are made with the code POISSON, PE2D and MDP.

In Fig. 4.5 and Fig. 4.6 b_2 and b_4 are plotted for magnets DRB005 and DRB006 for the calculations and measurements. The calculations are made with the code POISSON, PE2D and MDP.

In the case of magnets DRC007 and DRC008 the calculations are made with POISSON and PE2D. The computed and measured b_2 and b_4 are plotted in Fig. 4.7 and Fig. 4.8.

In Fig. 4.9 and Fig. 4.10 we have done the same comparison between the calculations and measurements for the magnet DRD009. The calculations are made with the code POISSON and PE2D.

Computed and measured b_2 in DRA001, DRA002 and DRA003

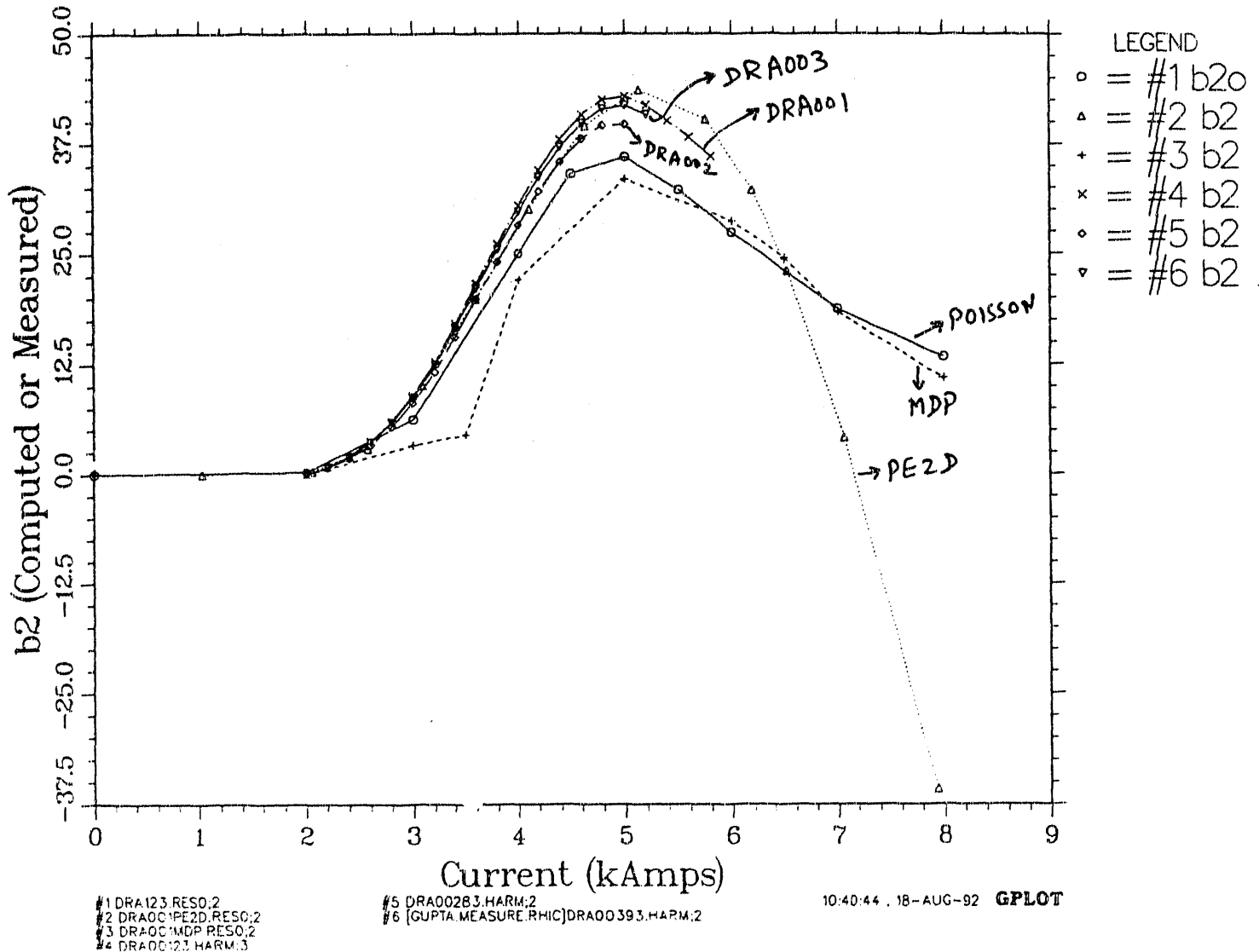


Figure 4.1: Computed and measured b_2 variation as a function of current in the 80 mm aperture RHIC arc dipole magnets DRA001, DRA002 and DRA003. These three magnets are made with the same iron cross section. The calculations are made with the codes POISSON, PE2D and MDP.

Computed and measured b_4 in DRA001, DRA002 and DRA003

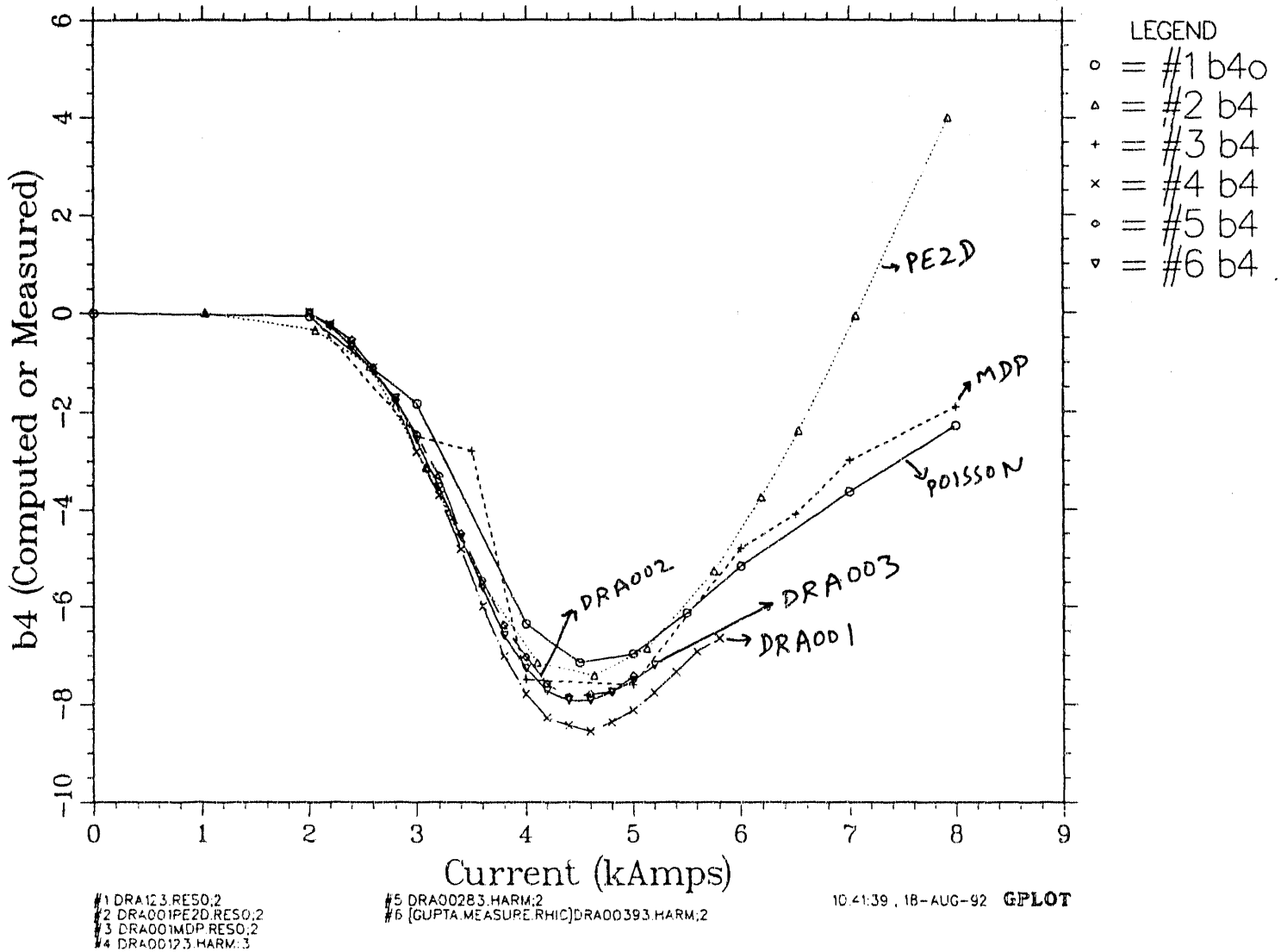


Figure 4.2: Computed and measured b_4 variation as a function of current in the 80 mm aperture RHIC arc dipole magnets DRA001, DRA002 and DRA003. These three magnets are made with the same iron cross section. The calculations are made with the codes POISSON, PE2D and MDP.

Computed and measured b_2 in DRA004

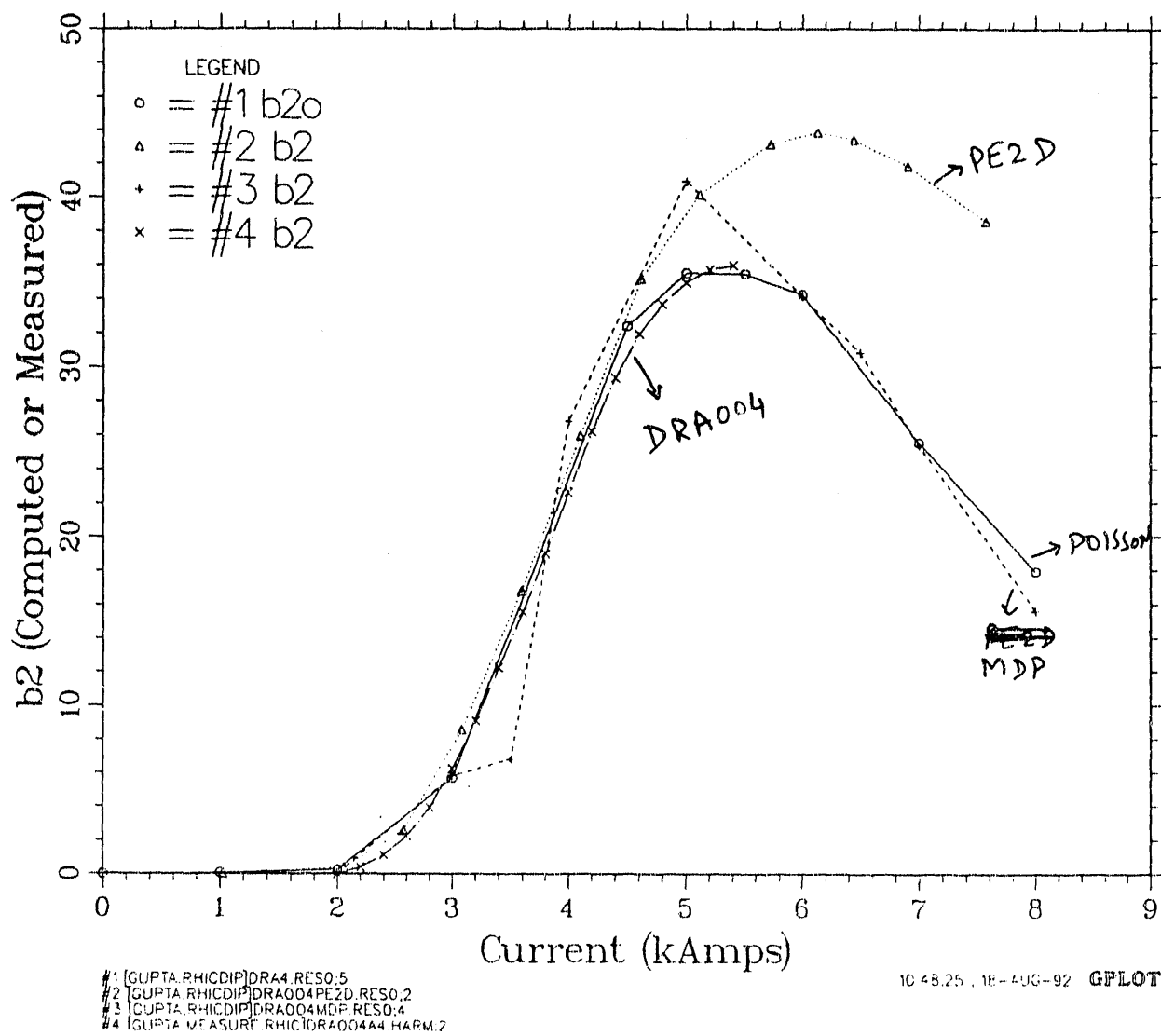


Figure 4.3: Computed and measured b_2 variation as a function of current in the 80 mm aperture RHIC arc dipole magnet DRA004. The calculations are made with the codes POISSON, PE2D and MDP.

Computed and measured b_4 in DRA004

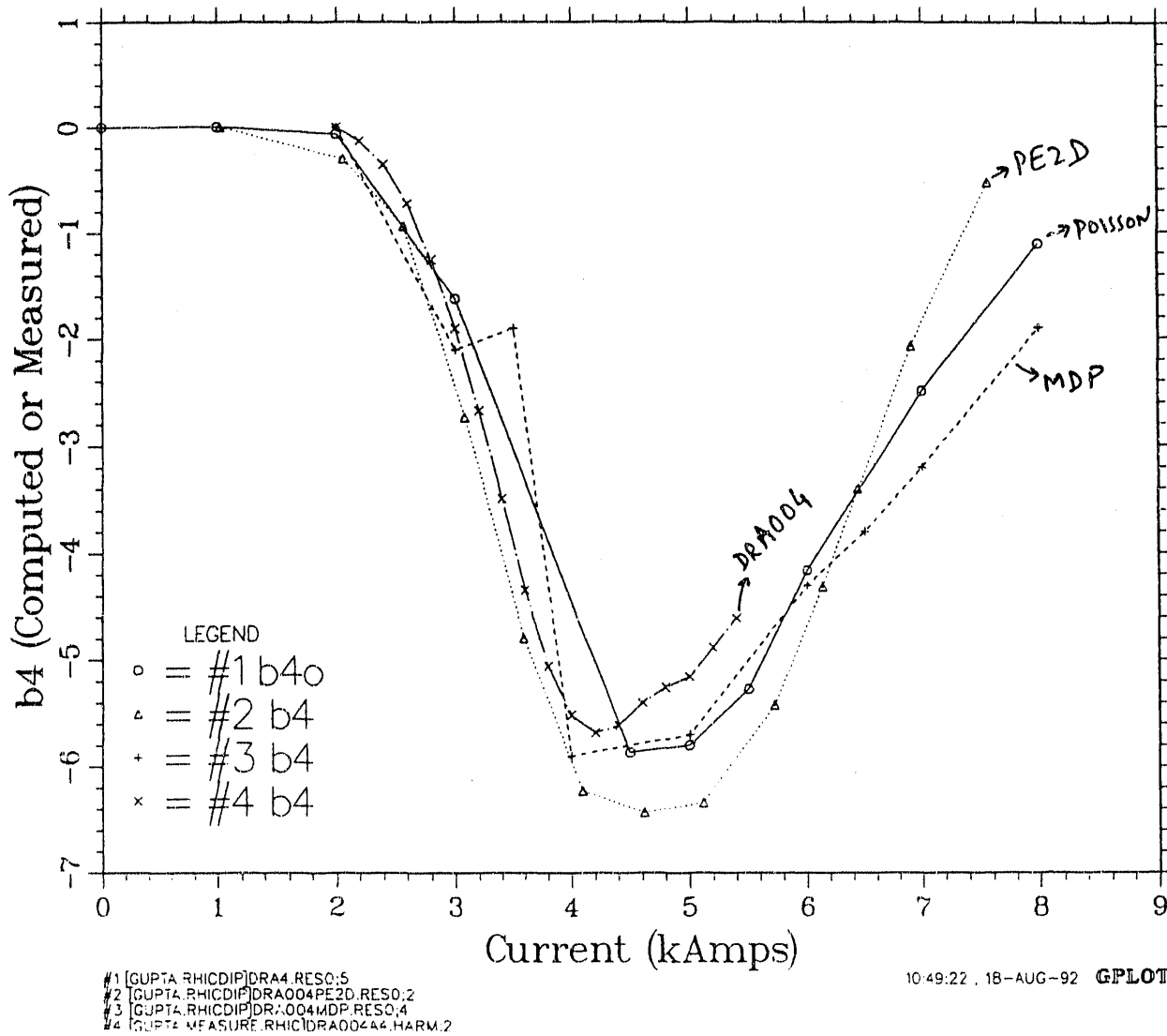


Figure 4.4: Computed and measured b_4 variation as a function of current in the 80 mm aperture RHIC arc dipole magnet DRA004. The calculations are made with the codes POISSON, PE2D and MDP.

Computed and measured b_2 in DRB005 and DRB006

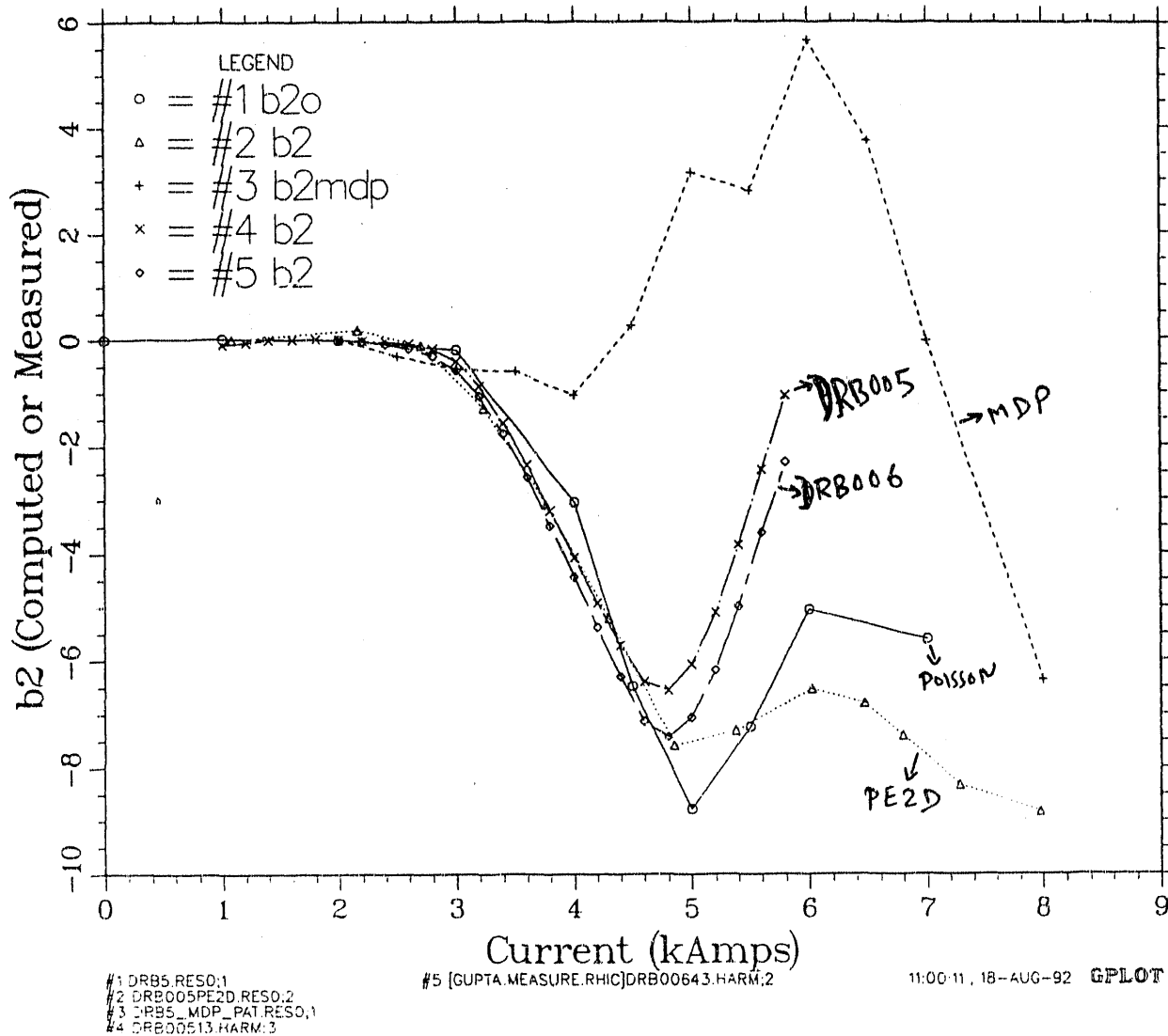


Figure 4.5: Computed and measured b_2 variation as a function of current in the 80 mm aperture RHIC arc dipole magnets DRB005 and DRB006. These two magnets are made with the same iron cross section. The calculations are made with the codes POISSON, PE2D and MDP.

Computed and measured b_4 in DRB005 and DRB006

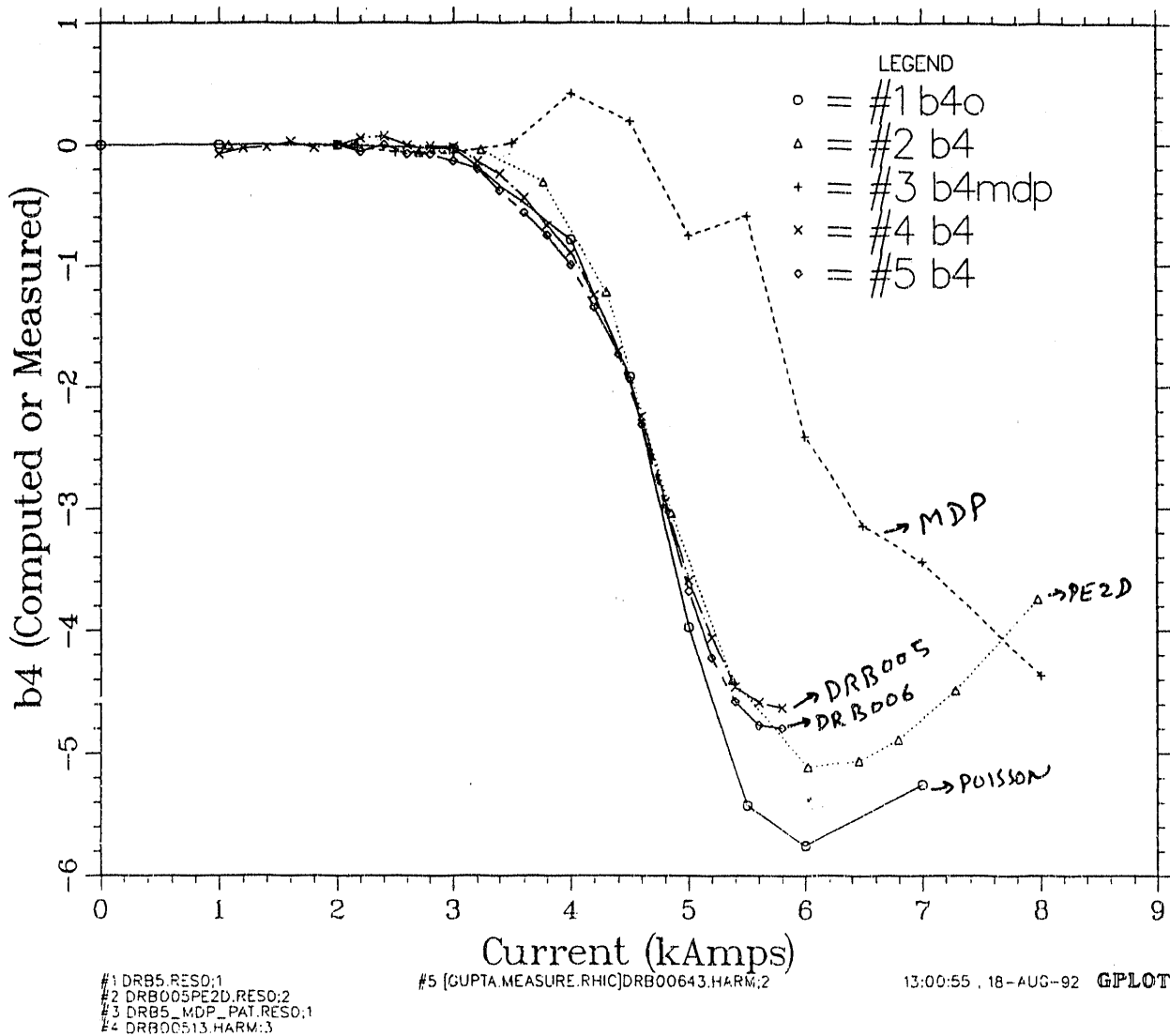


Figure 4.6: Computed and measured b_4 variation as a function of current in the 80 mm aperture RHIC arc dipole magnets DRB005 and DRB006. These two magnets are made with the same iron cross section. The calculations are made with the codes POISSON, PE2D and MDP.

Computed and measured b_2 in DRC007 and DRC008

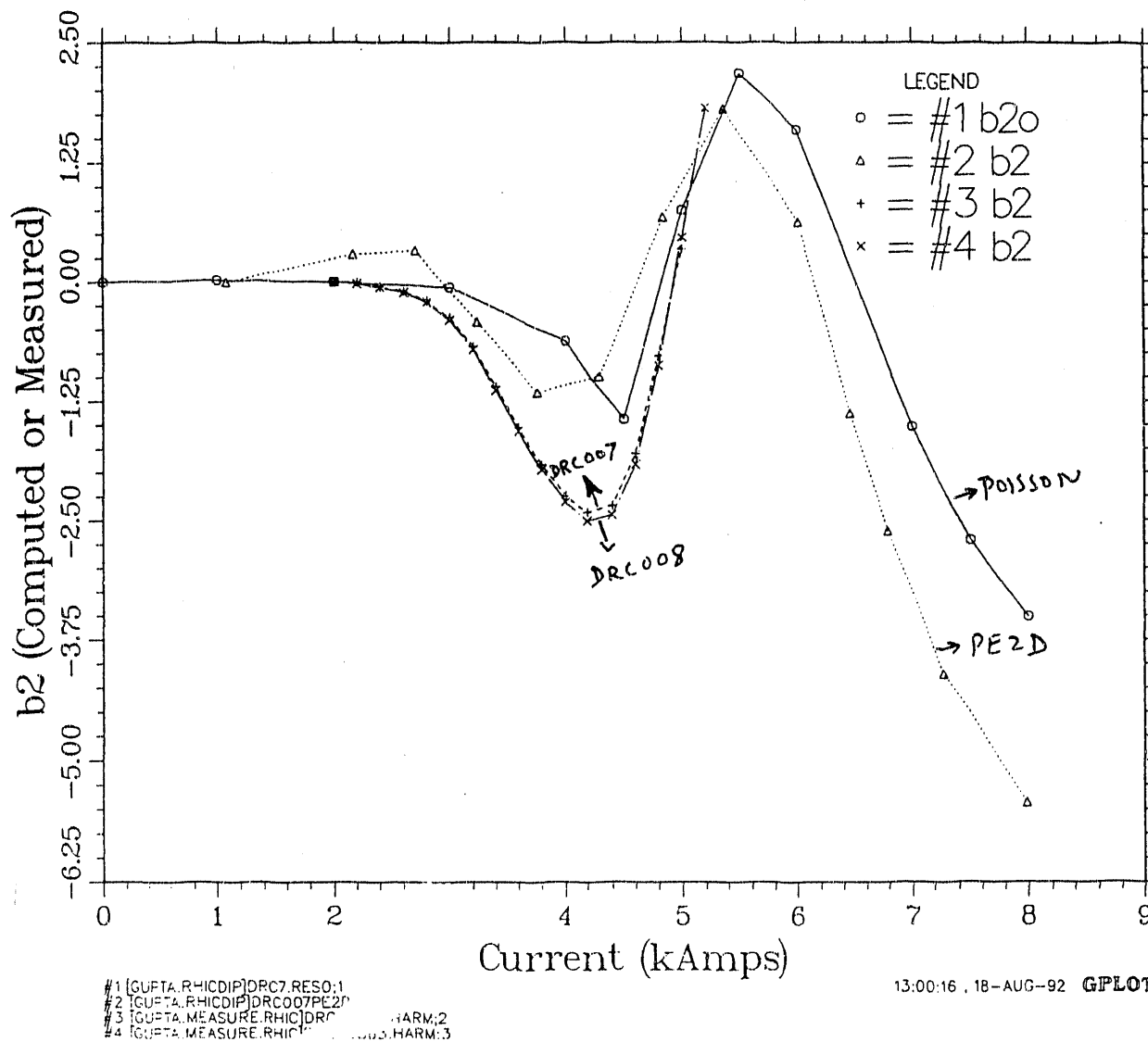


Figure 4.7: Computed and measured b_2 variation as a function of current in the 80 mm aperture RHIC arc dipole magnets DRC007 and DRC008. These two magnets are made with the same iron cross section. The calculations are made with the codes POISSON and PE2D.

Computed and measured b_4 in DRC007 and DRC008

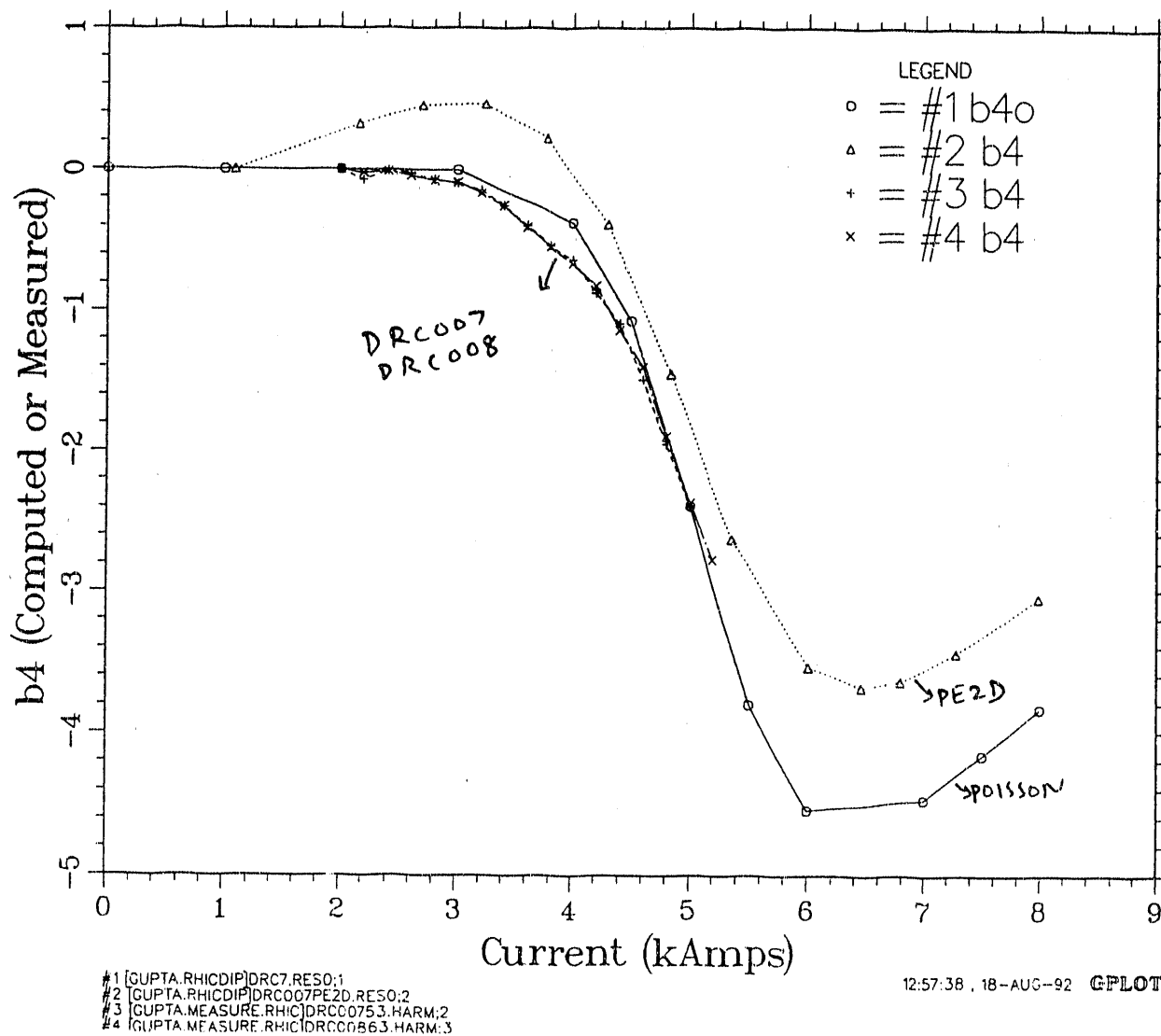


Figure 4.8: Computed and measured b_4 variation as a function of current in the 80 mm aperture RHIC arc dipole magnets DRC007 and DRC008. These two magnets are made with the same iron cross section. The calculations are made with the codes POISSON and PE2D.

Computed and measured b_2 in DRD009

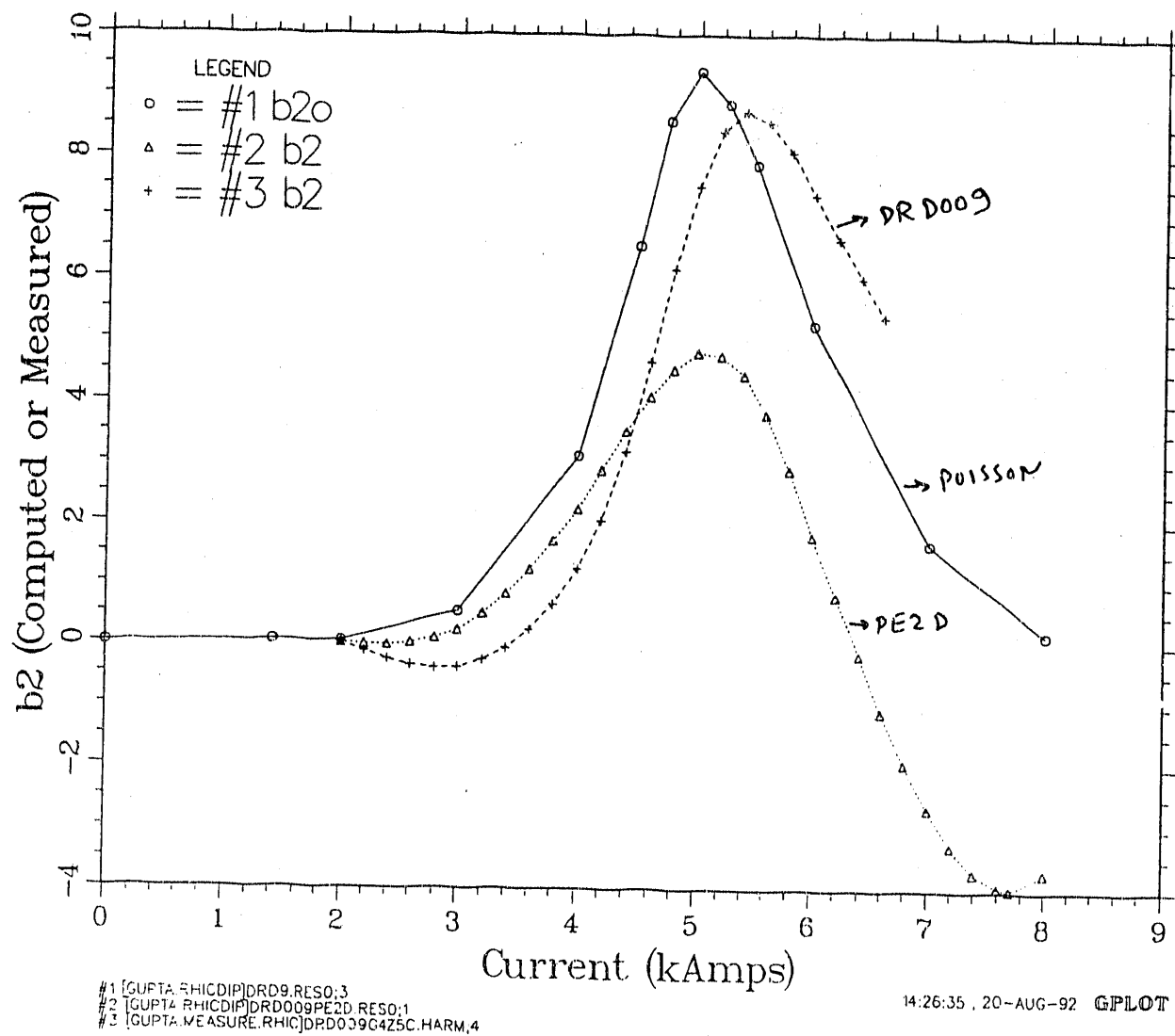


Figure 4.9: Computed and measured b_2 variation as a function of current in the 80 mm aperture RHIC arc dipole magnet DRD009. The calculations are made with the codes POISSON and PE2D.

Computed and measured b_4 in DRD009

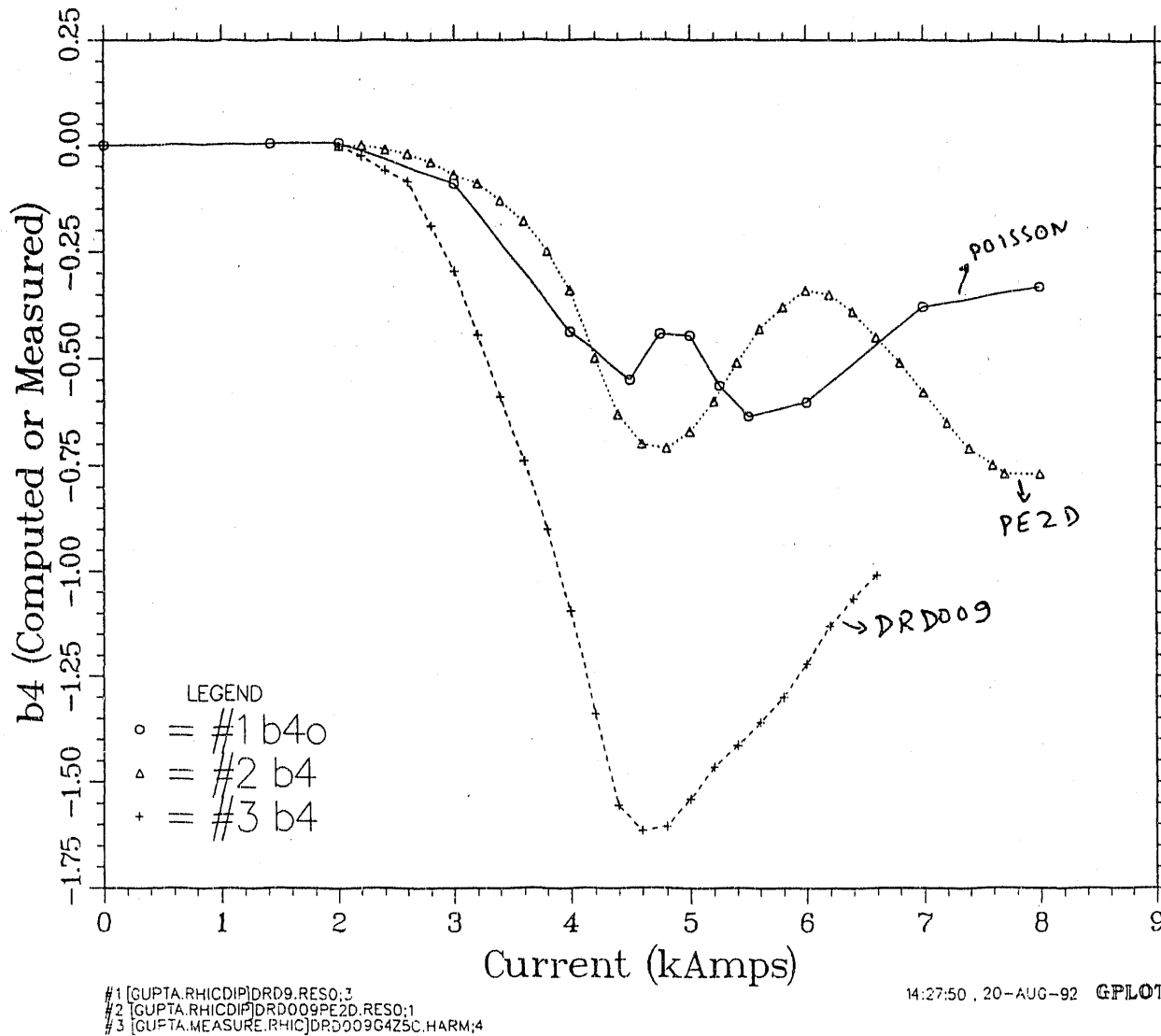


Figure 4.10: Computed and measured b_4 variation as a function of current in the 80 mm aperture RHIC arc dipole magnet DRD009. The calculations are made with the codes POISSON and PE2D.

5. DRE cross section

For the sake of completeness, we present the expected and computed harmonics in the next series of long magnets DRE011 and DRE012. The only difference in the yoke design between DRD009 and DRE011 is the presence of a $\frac{3}{8}$ " diameter saturation suppressor hole at a radius of 7.5 cm and at an angle of 33° degree. It has been described in detail in reference 5. Computed harmonics are obtained from the POISSON calculations and the expected harmonics are obtained by first taking the measured harmonics in the magnet DRD009, and then empirically adding to them the differences between the calculations and measurements in DRD009. The results are given in Fig. 5.1.

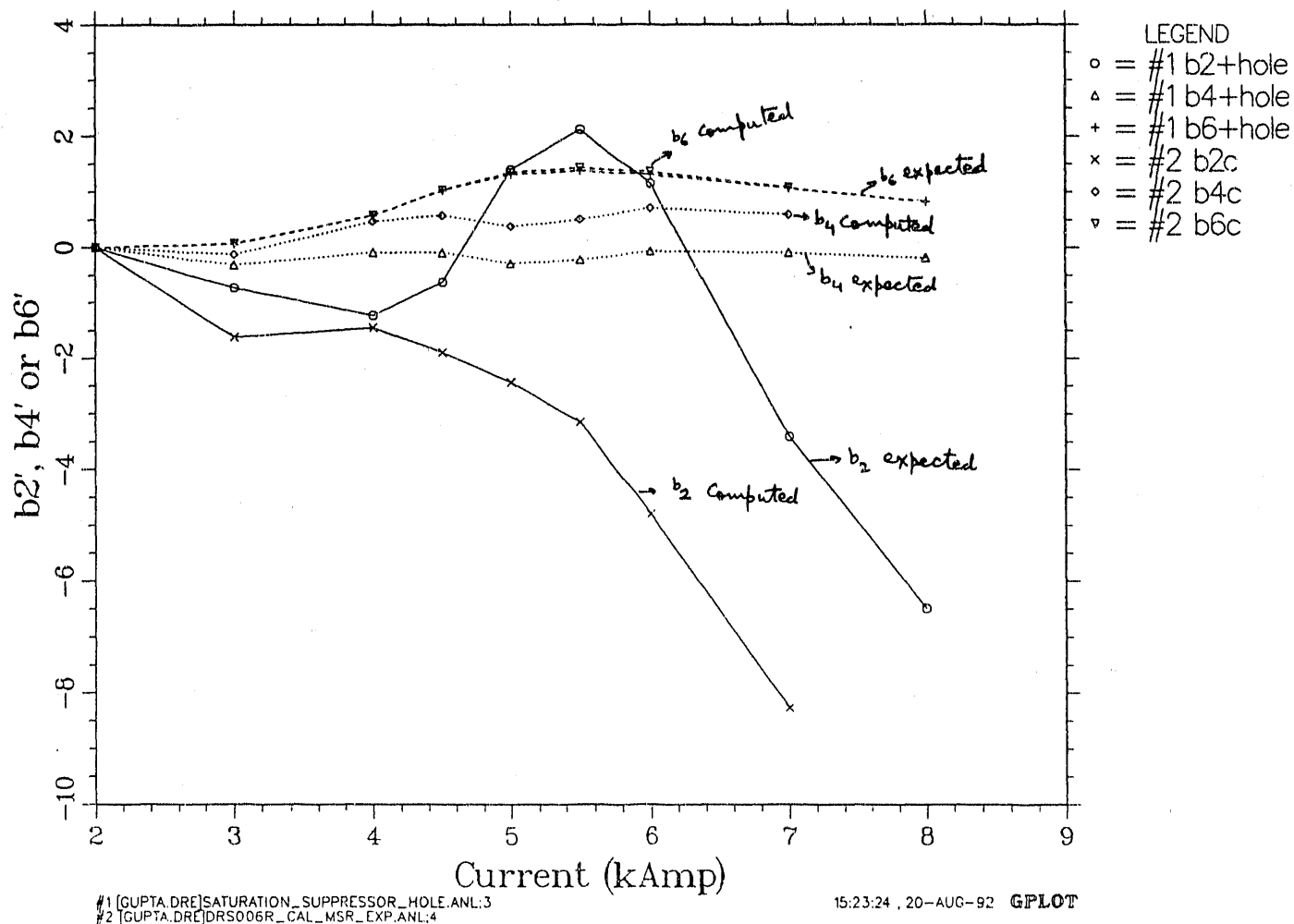


Figure 5.1: Expected and computed saturation induced harmonics in the long dipole DRE011 with saturation suppressor hole. Computed harmonics are obtained from the POISSON calculations and the expected harmonics are obtained by first taking the measured harmonics in the magnet DRD009, and then empirically adding to them the differences between the calculations and measurements in DRD009.

6. Discussion

One can see from Fig. 2.1 that we have been able to reduce the current dependence of the sextupole harmonic (b_2) by over an order of magnitude between 2 kA and 5 kA. The value of design current in the arc dipole for RHIC operation is ~ 5 kA. In the first long magnet DRA001, the maximum variation in the b_2 harmonic between the 2 kA and 5 kA current was over 42 unit and in the most recent short magnet this variation is reduced to under 2 unit. In the long dipole magnet DRE011, we expect this to be under 2 unit as well. Similarly one can see from Fig. 2.2 that b_4 variation has also been reduced by over an order of magnitude between 2 kA and 5 kA. In the first long magnet DRA001, the maximum variation in the b_4 harmonic between the 2 kA and 5 kA current was over 8 unit and in the most recent short magnet this variation is reduced to under 1/2 unit. In the long dipole magnet DRE011, we expect the current dependent variation in the b_4 harmonic to be under 1/2 unit as well. In the following paragraph we shall discuss what has been done to achieve this. We shall only discuss the features which were important from the iron saturation point of view only and mechanical changes in the design would be ignored.

DRA001, DRA002 and DRA003 dipoles were constructed by BBC. They had a 5mm radial gap between coil and yoke and had a notch at the pole location. A small gap and a pole notch both give a large iron saturation and hence we had over 42 unit of b_2 harmonic and -8 unit of b_4 . DRA004 had the same basic feature except for some small changes near the outer surface of iron. These changes do not alter the iron saturation significantly.

To reduce iron saturation, the radial gap between the coil and yoke was increased from 5mm to 10mm and the coil-yoke locating notch was moved from pole to midplane in the magnets DRB005 and DRB006. This brought b_2 saturation down from +42 unit to -6 unit and b_4 saturation from -8.5 unit to -3.6 unit. As before, these are the maximum deviation between 2 kA and 5 kA. This magnet had a non-magnetic stainless steel yoke midplane key. In the magnets DRC007 and DRC008, the material of this key was changed from non-magnetic stainless steel key to magnetic low carbon steel key. This change reduced b_2 saturation to -2.5 unit and b_4 saturation to -2.4 unit. In between a short magnet was built where the 5 mm midplane notch was modified to a 5mm iron tooth. That reduced b_2 saturation to +8 unit and b_4 to -1.1 unit. However, the tooth idea was not adopted in DRC007 because of its mechanical complications.

Neither the midplane notch nor the tooth (better magnetically but worse mechanically) was preferred for the production magnets. It is believed that a pole locating notch would be better able to define the pole location of the coil. As mentioned earlier, pole notch is bad magnetically. That in itself would make an already unacceptable saturation worse.

Therefore, a detailed study was undertaken to modify the cross section to significantly change the magnetics of the yoke with the desired mechanical properties. After considering a large number of variations, the one chosen for DRD009 was the one in which the location of the bypass hole was changed. This, with a pole notch and stainless steel key, actually improved the iron saturation (in b_4 harmonic) relative to DRB005 instead of making it worse. The b_2 saturation became +7 unit and b_4 -1.3 unit.

Finally a small saturation suppressor hole was added to practically eliminate all b_2 and b_4 saturation in DRE011 cross section. Before we discuss that, let us examine the differences between the calculations and measurements as they are given in Table 6.1. These calculations are done with the code POISSON and they ignore cryostat. Typically, at 5 kA cryostat induced b_2 is $\sim +1.5$ unit and b_4 is ~ -0.1 unit. Moreover, as mentioned earlier, the calculations are done only for the saturation induced harmonics and the harmonics due to coil deformation as a result of the Lorentz force on the coil are ignored. We have also ignored a small gap (of the order of 10 mil) between the top and bottom halves of the yokes. Some calculations show that this may give as much of 2 units of b_2 and 0.2 units of b_4 at 5 kA.

In Table 6.1, we have also given the maximum change in the measured values of b_2 and b_4 harmonics till 5 kA. The difference between the calculations and measurements did not bother much when the actual value of the saturation induced harmonic was large. However, at this stage they did matter as the target to make those harmonic became so small. The target was to make b_2 saturation less than 2 unit and b_4 saturation less than $\frac{1}{2}$ unit. This is within the difference between the calculations and measurements. Therefore, we empirically cancel out these small unexplained differences between the calculations and measurements (in this particular cross section) in arriving to an optimized location of the hole. The approach indeed worked as can be seen in Fig. 2.1 and Fig. 2.2 and described in detail in reference 4. In these figures please see curves marked for DRS6R where DRS6R represents the short dipole "*DRS006 rebuilt with the saturation suppressor holes*".

Table 6.1: The measured, computed and the difference between the two in the values of b_2 and b_4 harmonics at 5 kA relative to 2 kA value (i.e., value at 5 kA - value at 2 kA) in RHIC long magnets built to date. These calculations are done with the code POISSON and they ignore cryostat. Typically, at 5 kA cryostat induced b_2 is $\sim+1.5$ unit and b_4 is ~-0.1 unit.

Magnet name	b_2 Measured	b_2 Computed	difference Msr-Cal	b_4 Measured	b_4 Computed	difference Msr-Cal
DRA001	42.8	36.0	+6.8	-8.1	-7.0	-1.1
DRA002	39.7	36.0	+3.7	-7.4	-7.0	-0.4
DRA003	41.8	36.0	+5.8	-7.5	-7.0	-0.5
DRA004	34.5	35.5	-1.1	-5.2	-5.8	+0.6
DRB005	-6.1	-8.8	+2.7	-3.6	-4.0	+0.4
DRB006	-7.1	-8.8	+1.7	-3.7	-4.0	+0.3
DRC007	0.4	0.8	-0.4	-2.4	-2.4	0.0
DRC008	0.5	0.8	-0.3	-2.4	-2.4	0.0
DRD009	7.3	9.4	-2.1	-1.2	-0.4	-0.8

7. References

1. P.A. Thompson, et.al., "Iron saturation control in RHIC dipole magnets", Presented at 1991 Particle Accelerator Conference.
2. Testing and Measurement Group Notes describing the results of magnetic measurements.
3. P.A. Thompson, Magnet Division Notes describing design and comparing calculations with measurements.
4. R. Gupta, "DRS006 with Saturation Suppressor Holes", Magnet Division Note No. 457-16 (RHIC-MD-165), July 28, 1992.
5. R. Gupta, "Reducing iron saturation in arc dipoles with a saturation suppressor hole", Magnet Division Note No. 447-16 (RHIC-MD-158), June 10, 1992.

END

**DATE
FILMED**

11 / 5 / 92

